1963

Parametric devices using magnetic thin film and thin disks of yttrium iron garnet

Jerome George Doidge
Iowa State University

PARAMETRIC DEVICES USING MAGNETIC THIN FILM AND THIN DISKS OF YTTRIUM IRON GARNET

by

Jerome George Doidge

A Dissertation Submitted to the
Graduate Faculty in Partial Fulfillment of
The Requirements for the Degree of
DOCTOR OF PHILOSOPHY

Major Subject: Electrical Engineering

Approved:

Signature was redacted for privacy.

In Charge of Major Work

Signature was redacted for privacy.

Head of Major Department

Signature was redacted for privacy.

Dean of Graduate College

Iowa State University
Of Science and Technology
Ames, Iowa

1963

TABLE OF CONTENTS

I. INTRODUCTION

The thin magnetic film, with uniaxial anisotropy, has been investigated quite extensively in regard to its applications in electronic devices at frequencies up to 100 mc. Extensive work has also been carried out in the applications of ferrites and garnets in the X band range. The frequency ranges, such as L band, are becoming more important and their use in communications is being investigated. One of the main problems is the construction of devices that perform efficiently in this frequency range.

The primary purpose of this investigation is to study the adaptibility of thin magnetic films and thin disks of yttrium iron garnet, YIG, to this frequency range. The devices selected for this investigation were the harmonic generator and the parametric amplifier. The harmonic generator utilizes the non-linear properties of the magnetic material. If the magnetic material is biased along its easy or preferred axis of magnetization and if a magnetic field is applied perpendicular to the easy axis at a frequency corresponding to the resonant frequency for the particular bias, the magnetization vector will precess at a relatively large angle about the easy axis resulting in the generation of the harmonics of the applied field. The larger the applied field the greater the magnitude

of the harmonic terms until saturation effects start limiting the output.

In the parametric amplifier a field called the pump field is applied along the easy or preferred axis of the magnetic material. A dc bias is also applied along this direction. A field called the signal field is applied perpendicular to the bias direction. The signal field interacts with the pump field causing the generation of fields at the sum and difference of the frequencies of two fields and also fields at $n\omega_p \pm \omega_s$ where ω_p is the pump field and ω_s is the signal field. If the field corresponding to the difference between the pump and the signal field interacts with the pump field the difference is again generated which corresponds to the signal field and makes amplification of the signal field possible.

A general equation of motion based on the gyromagnetic properties of the electron can be developed for a magnetic material. If a dc magnetic field is applied to a free electron, this field will create a perpendicular torque which will cause the electron to precess about the field. If the electrons are all aligned so that their magnetic moments add they can be represented by a total magnetization vector M which precesses about its axis.

In the equation of motion the precession angle is assumed to be small and the magnetization vector is assumed to precess in a very flat ellipsoid in the plane of the magnetic material

because of the shape of the sample. If the magnetic material is in the shape of a flat disk with the diameter of the disk very much greater than the thickness of the material, strong magnetic fields called demagnetizing fields will be present perpendicular to the plane of the material and will essentially constrain the magnetization vector to lie in the plane of the material.

Magnetic crystals have preferred orientations, that is, there is an axis in the crystal about which the magnetization tends to align. This is also true in the case of the highly polycrystalline thin films of permalloy because of long range ordering. The reason for the geometric shape of the material is to reduce the bias necessary for the complete magnetization of the material.

If an rf field is applied perpendicular to the axis of the magnetization vector it will modulate its precession. For a certain value of bias the precessional motion will coincide with the motion due to the rf field resulting in a large precessional angle and a maximum amount of energy being absorbed from the rf field by the magnetic material.

In the analysis to follow the general equation of motion will be solved analytically and the calculated results compared with the experimental.

II. HARMONIC RELATIONSHIP USING THE LANDAU LIFSHITZ EQUATION

In this section the Landau Lifshitz equation of motion will be solved in terms of the susceptibility tensor χ and the relationship between second harmonic components and the applied field will be derived. In the literature the susceptibility tensor is usually derived using the cgs system of units instead of the rationalized mks system. The cgs system of units will be used in this section to coincide with the general literature.

Referring to Figure 1B, the undamped equation of motion of the spinning electron of angular momentum $\overline{J}$ and magnetic moment per unit volume $\overline{M}$ in a magnetic field is

$$\frac{d\overline{J}}{dt} = \overline{T} \tag{1}$$

where $\overline{T}$ is the torque exerted by the magnetic field. The torque $\overline{T}$ is related to the magnetic moment by

$$\overline{T} = \overline{M} \times \overline{H} \tag{2}$$

where $\overline{H}$ is the magnetic field. Also the angular momentum $\overline{J}$ is given by

$$\overline{J} = \frac{\overline{M}}{\gamma} \tag{3}$$

where γ is the magnetomechanical ratio equal to $-ge/2mc$, g being the Lande g factor, e the absolute value of the charge,

m the mass of the electron, and c the velocity of light. Hence

$$\frac{d\bar{M}}{dt} = \gamma \bar{M} \times \bar{H} \tag{4}$$

The magnetic field $\bar{H}$ is the vector sum of all magnetic fields seen by the spinning electron. It is necessary in ferromagnetic-resonance experiments to apply an rf magnetic field perpendicular to the dc field. Let

$$\bar{H} = \bar{H}_i + \bar{h}e^{j\omega t} \tag{5}$$

where $\bar{H}_i$ is the vector sum of the dc magnetic fields within the material including the applied dc field $\bar{H}_o$. The second term is the rf field term whose time dependance is $e^{j\omega t}$.

The condition for resonance is that the driving frequency ω equal the natural precession frequency ω_o. This fact will be shown in the following mathematical derivation. At resonance the oscillating component of torque will be in phase with the precessional motion of the magnetic dipole caused by the constant magnetic field of the steady state condition. The amplitude of the precession will grow causing energy to be absorbed by the electron from the applied field. Energy will be absorbed by the electrons at $\omega \neq \omega_o$ but the maximum energy is absorbed when $\omega = \omega_o$. The amplitude of precession is limited by damping which will be discussed later.

Figure 1A. The schematic representation of a thin magnetized disk of magnetic material illustrating the coordinate system and applied magnetic fields used in the accompanying analysis

Figure 1B. The schematic representation of the spinning electron under the influence of a bias field

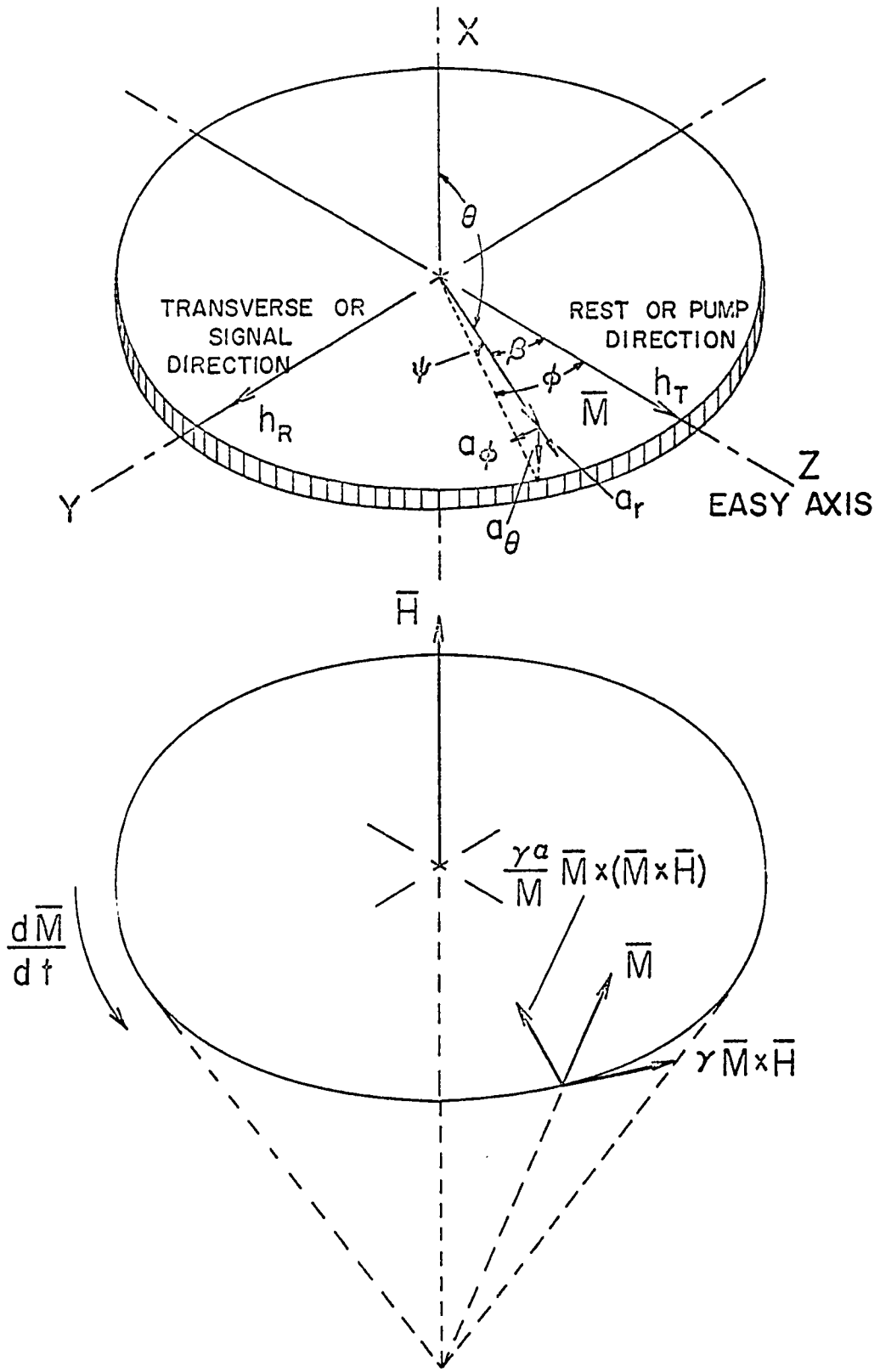
X
θ
TRANSVERSE OR
SIGNAL
DIRECTION
REST OR PUMP
DIRECTION
ψ
β
φ
h_T
h_R
$\bar{M}$
a_ϕ
Y
Z
EASY AXIS
a_r
a_θ
$\bar{H}$
$\frac{d\bar{M}}{dt}$
$\frac{\gamma a}{M}\,\bar{M}\times(\bar{M}\times\bar{H})$
$\bar{M}$
$\gamma\,\bar{M}\times\bar{H}$

The magnetization can be represented by

$$\bar{M} = \bar{M}_o + \bar{m}_1 e^{j\omega t} + \bar{m}_2 e^{j2\omega t} + \cdots + \tag{6}$$

where $\bar{M}_o$ is the steady state dc magnetization at a temperature below the Neél temperature. It is assumed that $\bar{H}_i \gg \bar{h}$ and $\bar{M}_o \gg \bar{m}$. It is also assumed that $\bar{H}_o$ and $\bar{M}_o$ lie in the Z direction where $\bar{H}_o$ is the dc applied field.

In the preliminary derivation of the susceptibility tensor it will be assumed that the medium is infinite in extent and that the anisotropy component of H_i is zero. The demagnetization and anisotropy terms will be added later. Therefore, for now let $\bar{H}_i = \bar{H}_o$. Considering that

$$\gamma(\bar{M}_o \times \bar{H}_o) = 0 \tag{7}$$

and substituting equations 5, 6, and 7 into equation 4 and simplifying results in

$$\begin{aligned} j\omega m_x &= \gamma(m_y H_o - M_o h_y) \\ j\omega m_y &= \gamma(M_o h_x - m_x H_o) \\ j2\omega m_z &= \gamma(m_x h_y - m_y h_x) \end{aligned} \tag{8}$$

In the first two equations of 8 the products of $m_y h_z$ and $m_x h_y$ have been neglected as small in comparison to the other terms.

The first two equations of 8 can be solved for m_x and m_y as

$$m_x = \frac{\gamma^2 M_o H_o h_x - j\omega\gamma M_o h_y}{\gamma^2 H_o^2 - \omega^2}$$

$$m_y = \frac{\gamma^2 M_o H_o h_y + j\omega\gamma M_o h_x}{\gamma^2 H_o^2 - \omega^2} \qquad (9)$$

It can be seen that the magnetization vector m has a singularity when

$$\omega = \gamma H_o = \omega_o \qquad (10)$$

Equation 9 can be written as

$$m_x = \frac{\gamma(\omega_o h_x - j\omega h_y) M_o}{\omega_o^2 - \omega^2}$$

$$m_y = \frac{\gamma M_o(\omega_o h_y + j\omega h_x)}{\omega_o^2 - \omega^2} \qquad (11)$$

The susceptibility tensor χ is defined by the relation

$$4\pi\bar{m} = \bar{\bar{\chi}} \cdot \bar{h} \qquad (12)$$

From equation 9 it is seen that

$$\chi_{xx} = \frac{\omega_m \omega_o}{\omega_o^2 - \omega^2} = \chi_{yy}$$

$$\chi_{yx} = \frac{j\omega_m \omega}{\omega_o^2 - \omega^2} = -\chi_{xy} \tag{13}$$

where the substitution has been made that

$$4\pi\gamma M_o = \omega_m \tag{14}$$

An alteration must be made in the tensor components to take losses into consideration. A loss term must exist in order to prevent the precessional motion from increasing without limit at resonance. The magnetic loss mechanisms contributing to the damping term are not completely understood. The loss is usually represented phenomenologically in the equations of motion.

The Landau Lifshitz form of the equation of motion will be used in this derivation. In this derivation it is assumed that the magnitude of M is a constant of the motion. The Landau Lifshitz equation of motion (12) is

$$\frac{d\bar{M}}{dt} = \gamma(\bar{M} \times \bar{H}) - \lambda\left[\frac{(\bar{H}\cdot\bar{M})\bar{M}}{M^2} - \bar{H}\right] \tag{15}$$

where λ is a damping factor having dimensions of frequency and is called the relaxation frequency. Equation 15 can be rearranged in the form (9)

$$\frac{d\bar{M}}{dt} = \gamma(\bar{M} \times \bar{H}) - \frac{\gamma\alpha}{M}\left[\bar{M} \times (\bar{M} \times \bar{H})\right] \tag{16}$$

where $\frac{\gamma\alpha}{M} = \frac{\lambda}{M^2}$. The factor α is known as the phenomenological damping constant. Taking the cross product of M with equation 16 and neglecting the terms in α^2 results in

$$\dot{\bar{M}} = \gamma(\bar{M} \times \bar{H}) - \frac{\alpha}{M} (\bar{M} \times \dot{\bar{M}}) \tag{17}$$

where $\frac{dM}{dt}$ is represented by $\dot{M}$.

Following the same procedure as used in the undamped case

$$j\omega\bar{m} = \gamma(\bar{M}_o \times \bar{h}) - \gamma(\bar{H}_i \times \bar{m}) - j\frac{\omega\alpha}{M}(\bar{M}_o \times \bar{m}) =$$

$$\gamma(\bar{M}_o \times \bar{h}) + (\omega_o + \tfrac{j}{T}) (\bar{m} \times \bar{i}_z) \tag{18}$$

where $\alpha = \frac{1}{\omega T}$ and $\bar{i}_z$ is the unit vector in the z direction. The only difference between equation 18 and the equation of the undamped case is that now

$$\omega_o + \tfrac{j}{T} = \gamma H_i \tag{19}$$

If $\omega_o + \frac{j}{T}$ is substituted for ω_o in the components of the susceptibility tensor for the undamped case the components for the damped case become

$$\chi_{xx} = \chi_{yy} = \frac{(\omega_o + \frac{j}{T})\omega_m}{(\omega_o + \frac{j}{T})^2 - \omega^2}$$

$$\chi_{yx} = -\chi_{xy} = \frac{j\omega\omega_m}{(\omega_o + \frac{j}{T})^2 - \omega^2} \tag{20}$$

The susceptibility tensor components can be separated into real and imaginary parts and represented as

$$\chi_{xx} = \chi'_{xx} - j\,\chi''_{xx}$$

$$\chi_{xy} = -\chi''_{xy} - j\,\chi'_{xy} \tag{21}$$

From equation 20 these components become

$$\chi'_{xx} = \frac{\omega_m \omega_o \left[\omega_o^2 - \omega^2 + \frac{1}{T^2}\right]}{\left[\omega_o^2 - \omega^2 - \frac{1}{T^2}\right]^2 + 4\,\frac{\omega_o^2}{T^2}}$$

$$\chi''_{xx} = \frac{\omega_m}{T}\,\frac{\left[\omega_o^2 + \omega^2 + \frac{1}{T^2}\right]}{\left[\omega_o^2 - \omega^2 - \frac{1}{T^2}\right]^2 + 4\,\frac{\omega_o^2}{T^2}}$$

$$\chi''_{xy} = \frac{-\omega_m \omega_o \omega \frac{1}{T}}{\left[\omega_o^2 - \omega^2 - \frac{1}{T^2}\right]^2 + \frac{4\,\omega_o^2}{T^2}}$$

$$\chi'_{xy} = \frac{\omega_m \omega \left[\omega_o^2 - \omega^2 - \frac{1}{T^2}\right]}{\left[\omega_o^2 - \omega^2 - \frac{1}{T^2}\right]^2 + \frac{4\,\omega_o^2}{T^2}} \tag{22}$$

The components χ'_{xx} and χ'_{xy} are dispersive terms while the

χ''_{xx} and χ''_{xy} components represent dissipative terms.

The magnetic susceptibility has been solved for an infinite medium. To account for a finite sample charge it would be necessary to solve an electromagnetic boundary value problem. If the sample size is small compared with a wavelength as it is for frequencies considered in this dissertation, the magnetic field inside the sample can be assumed to have uniform intensity but unequal to the field outside the sample. It is very difficult to determine the magnetic field inside an arbitrarily shaped sample. However, the problem has been worked out for a general ellipsoid and its limiting forms. The results are expressed in terms of demagnetizing factors. The internal field is given by $H_i = H_o - 4\pi N \cdot M$ where $4\pi N \cdot M$ is an opposing internal field due to the presence of dipoles on the sample surface. The N's satisfy the condition

$$N_x + N_y + N_z = 1 \tag{23}$$

For a very thin slab the value of the component of N perpendicular to the surface of the slab is equal approximately to 1 and the other components of N are equal to zero.

Taking into consideration both damping and demagnetization equation 8 now becomes

$$4\pi j\omega m_x = -\omega_m (h_y - N_y 4\pi m_y) + m_y 4\pi (\omega_o - \omega_m N_z + \tfrac{j}{T})$$

$$4\pi j\omega m_y = \omega_m (h_x - N_x 4\pi m_x) - m_x 4\pi(\omega_o - \omega_m N_z + \frac{j}{T})$$

$$j2\omega m_z = \gamma \left[m_x h_y - m_x h_y + m_x m_y 4\pi (N_x - N_y) \right] \qquad (24)$$

From the first two equations of equation 24 m_x and m_y can be obtained as

$$4\pi m_x = \frac{-j\omega\omega_m h_y + \omega_m h_x (\omega_o + \omega_m N_y)}{\omega_r^2 - \omega^2 - \frac{1}{T^2} + \frac{2j}{T}\left[\omega_o + (\frac{N_x + N_y}{2})\omega_m \right]} \qquad (25)$$

$$4\pi m_y = \frac{j\omega\omega_m h_x + \omega_m h_y (\omega_o + \omega_m N_y + \frac{j}{T})}{\omega_r^2 - \omega^2 - \frac{1}{T^2} + \frac{2j}{T}\left[\omega_o + \frac{(N_x + N_y)\omega_m}{2}\right]}$$

where

$$\omega_r^2 = \left[\omega_o + (N_x - N_z)\omega_m\right]\left[\omega_o + (N_y - N_z)\omega_m\right] \qquad (26)$$

The real and imaginary parts of the components of the susceptibility tensor can now be written as

$$\chi'_{xx} = \frac{\omega_m(\omega_r^2 - \omega^2 + \frac{1}{T^2})(\omega_o + \omega_m N_y) + \frac{\omega_m}{T^2}\left[2\omega_o + (N_x + N_y)\omega_m\right]}{(\omega_r^2 - \omega^2 - \frac{1}{T^2})^2 + \frac{4}{T^2}\left[\omega_o + (\frac{N_x + N_y}{2})\omega_m\right]^2}$$

$$\chi''_{xx} = \frac{\frac{\omega_m}{T}\left[\omega_r^2 + \omega^2 + \frac{1}{T^2} + \omega_m(N_y - N_x)(\omega_o + \omega_m N_y)\right]}{(\omega_r^2 - \omega^2 - \frac{1}{T^2})^2 + \frac{4}{T^2}\left[\omega_o + (\frac{N_x + N_y}{2})\omega_m\right]^2}$$

$$\chi''_{xy} = \frac{\frac{2\omega\omega_m}{T}\left[\omega_o + \left(\frac{N_x + N_y}{2}\right)\omega_m\right]}{\left(\omega_r^2 - \omega^2 - \frac{1}{T^2}\right)^2 + \frac{4}{T^2}\left[\omega_o + \left(\frac{N_x + N_y}{2}\right)\omega_m\right]^2}$$

$$\chi'_{xy} = \frac{\omega\omega_m\left(\omega_r^2 - \omega^2 - \frac{1}{T^2}\right)}{\left(\omega_r^2 - \omega^2 - \frac{1}{T^2}\right)^2 + \frac{4}{T^2}\left[\omega_o + \left(\frac{N_x + N_y}{2}\right)\omega_m\right]^2} \qquad (27)$$

The components of χ_{yy} are the same as the components of χ_{xx} except N_x is substituted for N_y.

If for a thin disk a dc magnetic field is applied parallel to the flat surface and in the z direction as shown in Figure 1A the results are

$$N_x \hat{=} N_z \hat{=} 0$$

$$N_y \hat{=} 1$$

$$\omega_r = \left[\omega\left(\omega_o + \omega_m\right)\right]^{\frac{1}{2}} = \gamma\left[B_o H_o\right]^{\frac{1}{2}}$$

$$\text{or } f_r = \frac{\gamma}{2\pi}\left[H_o\left(H_o + 4\pi M\right)\right]^{\frac{1}{2}} \qquad (28)$$

where B_o is the saturation value of the magnetic induction at the operating temperature of the magnetic material.

Suppose to the flat disk an essentially linear driving field h_y is applied in the y direction. The bias field

direction is along the easy or preferred axis of magnetization. Therefore, the applied magnetic field is perpendicular to the easy axis. The third equation of equation 24 now becomes

$$\frac{d(m_2)_z}{dt} = (\dot{m}_2)_z = \gamma(m_x h_y + 4\pi\, m_x m_y N_x) \tag{29}$$

where the time dependence of $(\dot{m}_2)_z$ is $e^{j2\omega t}$ or the term is at a frequency of twice the applied frequency. This second harmonic component of rf magnetization at resonance can be written as

$$4\pi(m_2)_z = \frac{\gamma(1 + N_x \chi''_{yy})\, \chi''_{xy} h_y^2}{2\omega} \tag{30}$$

Substituting for the susceptibility tensor components and noting on resonance $N_x\chi''_{yy} >> 1$ equation 30 can be written as

$$4\pi(m_2)_z = \frac{\gamma N_x \chi''_{yy}\, \chi''_{xy}\, h_y^2}{2\omega}$$

$$= \frac{\gamma\omega_m\left[2\omega^2 + \frac{1}{T^2} + \omega_m(\omega_o+\omega_m)\right]\left[\frac{2\omega\omega_m}{T}(\omega_o + \frac{\omega_m}{2})\right] h_y^2}{2\omega T\left[\frac{1}{T^4} + \frac{4}{T^2}(\omega_o + \frac{\omega_m}{2})^2\right]^2}$$

$$= \frac{\gamma\omega_m^2 T^2\left[2\omega^2 + \frac{1}{T^2} + \omega_m\omega\sqrt{1 + \frac{\omega_m}{\omega_o}}\right]\left[\omega_o + \frac{\omega_m}{2}\right] h_y^2}{\left[\frac{1}{T^2} + 4(\omega_o + \frac{\omega_m}{2})^2\right]^2} \tag{31}$$

The $\frac{1}{T^2}$ terms can be neglected as small in comparison to the rest of the terms. Therefore

$$4\pi(m_2)_z = \frac{\left(\frac{\gamma\omega_m Th_y^2}{4}\right)\left(\frac{\omega_m T}{2}\right)\left(2\omega^2+\omega_m\omega\sqrt{1+\frac{\omega_m}{\omega_o}}\right)(2\omega)}{\left(\omega_o+\omega\sqrt{1+\frac{\omega_m}{\omega_o}}\right)^3} \tag{32}$$

For the infinite meduim case the value of $4\pi(m_2)_z$ would be

$$\frac{\gamma\omega_m Th_y^2}{4}$$

which is smaller than for the case considered here. In fact the thin disk geometry represents the optimum shape for harmonic generation. The factor $\frac{\omega_m T}{2}$ is called the intrinsic figure of merit (13) for frequency doubling.

It can be seen from equation 32 that the second harmonic component is proportional to the square of the driving field. Hence the second harmonic power would be proportional to the square of the input power.

III. SOLUTION OF THE GENERAL EQUATION OF MOTION FOR THE PARAMETRIC AMPLIFIER

Equation 16 of part I can be written as

$$\dot{\bar{M}} = \gamma \bar{T} + \frac{\gamma \alpha}{M} \bar{M} \times \bar{T} \tag{33}$$

The torque T and the magnetization M can be represented in spherical coordinates as

$$\bar{T} = T_r \bar{a}_r + T_\theta \bar{a}_\theta + T_\phi \bar{a}_\phi$$

$$\bar{M} = M \bar{a}_r \tag{34}$$

where $\bar{a}_r$, $\bar{a}_o$, and $\bar{a}_\phi$ are the unit vectors in the r, θ, and ϕ directions respectively as shown in Figure 1A. The solution of the cross product of $\bar{M}$ and $\bar{T}$ is

$$\bar{M} \times \bar{T} = \begin{vmatrix} \bar{a}_r & \bar{a}_\theta & \bar{a}_\phi \\ M & 0 & 0 \\ T_r & T_\theta & T_\phi \end{vmatrix} = - MT_\phi \bar{a}_\theta + MT_\theta \bar{a}_\phi \tag{35}$$

Since the value of M is assumed constant $\dot{\bar{M}}$ can be written as

$$\dot{\bar{M}} = \frac{d}{dt} (M\bar{a}_r) = M \frac{d\bar{a}_r}{dt} \tag{36}$$

The expression for $\frac{d\bar{a}_r}{dt}$ is given by

$$\frac{d\bar{a}_r}{dt} = \frac{\partial \bar{a}_r}{\partial r} \frac{dr}{dt} + \frac{\partial \bar{a}_r}{\partial \theta} \frac{d\theta}{dt} + \frac{\partial a_r}{\partial \phi} \frac{d\phi}{dt}$$

$$= 0 + \bar{a}_\theta \dot{\theta} + \bar{a}_\phi \sin\theta \dot{\phi} \tag{37}$$

Substituting equation 37 into equation 36 the result is

$$\dot{\bar{M}} = M\,\dot{\theta}\,\bar{a}_{\theta} + M \sin\theta\,\dot{\phi}\,\bar{a}_{\phi} \tag{38}$$

Substituting equations 34, 35, 36, and 38 into equation 33 and equating vectors of like direction results in

$$M\dot{\theta} = \gamma T_{\theta} + \frac{\gamma\alpha}{M}\,(-MT_{\phi}) \tag{39}$$

in the $\bar{a}_{\theta}$ direction and

$$M \sin\theta\,\dot{\phi} = \gamma T_{\phi} + \frac{\gamma\alpha}{M}\,MT_{\theta} \tag{40}$$

in the $\bar{a}_{\phi}$ direction.

The force on a system of electrons can be represented by

$$\bar{F} = -\nabla E \tag{41}$$

where E is the total energy of the system. The torque on the system is

$$\bar{T} = \bar{r} \times \bar{F} = -\bar{r} \times \nabla E \tag{42}$$

where $\bar{r}$ is the radius vector in the direction of $\bar{M}$. Taking the gradient of E, using spherical coordinates, the torque becomes

$$\bar{T} = -\bar{r}X\left[\frac{\partial E}{\partial r}\,\bar{a}_{r} + \frac{1}{r}\,\frac{\partial E}{\partial \theta}\,a_{\theta} + \frac{1}{r \sin\theta}\,\frac{\partial E}{\partial \phi}\,a_{\phi}\right] \tag{43}$$

where $\bar{r} = r\,\bar{a}_r$.

Performing the cross product the expression for torque becomes

$$\bar{T} = \frac{1}{\sin\theta}\frac{\partial E}{\partial \phi}\,\bar{a}_\theta - \frac{\partial E}{\partial \theta}\,\bar{a}_\phi \tag{44}$$

Substituting for the components of $\bar{T}$ in equations 39 and 40 results in

$$M\dot{\theta} = \frac{\gamma}{\sin\theta}\frac{\partial E}{\partial \phi} + \alpha\gamma\frac{\partial E}{\partial \theta}$$

$$M \sin\theta\,\dot{\phi} = -\gamma\frac{\partial E}{\partial \theta} + \frac{\gamma\alpha}{\sin\theta}\frac{\partial E}{\partial \phi} \tag{45}$$

Referring to Figure 1A it can be seen that

$$\theta = \frac{\pi}{2} - \psi \tag{46}$$

Making a change of variable from θ to ψ results in

$$M\dot{\psi} = \frac{-\gamma}{\cos\psi}\frac{\partial E}{\partial \phi} + \gamma\alpha\frac{\partial E}{\partial \psi} \tag{47}$$

$$M\cos\psi\,\dot{\phi} = \frac{\gamma\partial E}{\partial \psi} + \frac{\gamma\alpha}{\cos\psi}\frac{\partial E}{\partial \phi}$$

The free energy of the system may be represented as

$$E = K\sin^2\beta + \frac{M^2}{2\mu_o}\sin^2\psi - \bar{H}_{app}\cdot\bar{M} \tag{48}$$

where the first term is the anisotropy term, the second term

is due to demagnetizing forces, and the third term is due to the interaction of the magnetization vector $\overline{M}$ with the applied field. The angle β is the angle between the easy axis and the magnetization vector M. Referring to Figure 1A it is seen that β can be expressed in terms of ψ and ϕ resulting in

$$\sin^2\beta = \sin^2\psi + \cos^2\psi \sin^2\phi \tag{49}$$

Referring again to Figure 1A it is seen that

$$M_z = M\cos\psi\cos\phi$$

$$M_y = M\cos\psi\sin\phi \tag{50}$$

Therefore

$$\overline{H}_{app} \cdot \overline{M} = MH_z \cos\psi\cos\phi + MH_y \cos\psi\sin\phi \tag{51}$$

The expression for the energy can now be written as

$$E = K(\sin^2\psi + \cos^2\psi \sin^2\phi) + \frac{M^2}{2\mu_o} \sin^2\psi \tag{52}$$

$$- MH_z \cos\psi\cos\phi - MH_y \cos\psi\sin\phi$$

It may be noted that the energy terms due to exchange forces, displacement and conduction currents, and also magnetostriction were neglected in the energy expression. These terms are considered negligible for the case considered.

Equation 52 can now be differentiated with respect to ψ and after a slight simplification becomes

$$\frac{\partial E}{\partial \psi} = M\sin\psi \left[\frac{2K}{M} \cos^2\phi \cos\psi + \frac{M}{\mu_o} \cos\psi + H_z \cos\phi + H_y \sin\phi \right] \tag{53}$$

If equation 52 is now differentiated with respect to ϕ and simplified the result is

$$\frac{\partial E}{\partial \phi} = M\cos\psi \left[\frac{2K}{M} \sin\phi \cos\psi + H_z \sin\phi - H_y \cos\phi \right] \tag{54}$$

Substituting equation 53 and 54 into equation 47 gives

$$M\dot{\psi} = -\gamma M \left[\frac{2K}{M} \sin\phi \cos\phi \cos\psi + H_z \sin\phi - H_y \cos\phi \right] + \gamma\alpha M \sin\psi \left[\frac{2K}{M} \cos^2\phi \cos\psi + \frac{M}{\mu_o} \cos\psi + H_z \cos\phi + H_y \sin\phi \right]$$

$$M\cos\psi\,\dot{\phi} = \gamma M \sin\psi \left[\frac{2K}{M} \cos^2\phi \cos\psi + \frac{M}{\mu_o} \cos\psi + H_z \cos\phi + H_y \sin\phi \right] + \gamma\alpha M \left[\frac{2K}{M} \sin\phi \cos\phi \cos\psi + H_z \sin\phi - H_y \cos\phi \right] \tag{55}$$

For the particular geometry considered here and for the materials considered

$$\frac{M}{\mu_o} >> \frac{2K}{M},\ H_z,\ \text{and}\ H_y$$

$$\cos\psi \cong 1$$

$$\sin\psi \cong \psi \tag{56}$$

Making use of these facts equation 55 becomes

$$\dot{\psi} = -\gamma\left[\frac{2K}{M}\sin\phi\cos\phi + H_z\sin\phi - H_y\cos\phi - \alpha\frac{M\psi}{\mu_o}\right]$$

$$\dot{\phi} = \gamma\left[\frac{M\psi}{\mu_o} + \alpha\left(\frac{2K}{M}\sin\phi\cos\phi + H_z\sin\phi - H_y\cos\phi\right)\right] \qquad (57)$$

To simplify equation 57 let

$$F = \frac{2K}{M}\sin\phi\cos\phi + H_z\sin\phi - H_y\cos\phi = \frac{1}{M}\frac{\partial E}{\partial\phi} \qquad (58)$$

Equation 57 may now be written as

$$\dot{\psi} = -\gamma F + \frac{\alpha\gamma M\psi}{\mu_o}$$

$$\dot{\phi} = \gamma\alpha F + \frac{\gamma M\psi}{\mu_o} \qquad (59)$$

Equation 59 agrees with the expressions obtained by Pohm and Olson (16) and Gillette and Oshima (10).

Equation 59 can now be differentiated with respect to time giving

$$\ddot{\phi} = \gamma\alpha\dot{F} + \frac{\gamma M}{\mu_o}\dot{\psi} = \gamma\left[\frac{M\dot{\psi}}{\mu_o} + \alpha\dot{F}\right] \cong \frac{\gamma M\dot{\psi}}{\mu_o} \qquad (60)$$

since $\alpha << \frac{M}{\mu_o}$ and it is assumed that $\dot{\psi}$ is of the same order of magnitude as $\dot{\phi}$. If the second equation of equation 59 is now multiplied by $-\alpha$ and added to the first equation of equation

59 the result is

$$\dot{\varphi} - \alpha\dot{\phi} = -\gamma F\ (1 + \alpha^2) \triangleq -\gamma F \tag{61}$$

Therefore

$$\dot{\varphi} = \alpha\dot{\phi} - \gamma F \tag{62}$$

Substituting equation 62 into equation 60 gives

$$\ddot{\phi} = \gamma\ (-\gamma\frac{MF}{\mu_o} + \alpha\dot{F} + \frac{\alpha M}{\mu_o}\dot{\phi}\ ) \tag{63}$$

Equation 63 agrees with the expression obtained by D. O. Smith (23).

If the term $\gamma\alpha\dot{F}$ is considered negligible with respect to the rest of the terms in equation 63 the resulting expression can be written as

$$\ddot{\phi} - \frac{\alpha\gamma M\dot{\phi}}{\mu_o} + \frac{\gamma^2 M}{\mu_o}\left[\frac{2K}{M}\sin\phi\cos\phi + H_z\sin\phi - H_y\cos\phi\right] = 0 \tag{64}$$

If it is assumed that the angle ϕ is always small the approximations $\sin\phi = \phi$ and $\cos\phi = 1$ can be made.

Considering these approximations equation 64 becomes

$$\ddot{\phi} - \frac{\alpha\gamma M\dot{\phi}}{\mu_o} + \frac{\gamma^2 M}{\mu_o}\left(\frac{2K}{M} + H_z\right)\phi = H_y\frac{\gamma^2 M}{\mu_o} \tag{65}$$

Equation 65 is the general equation of motion. This equation

will now be solved using different methods to obtain an expression for $\dot{\phi}$.

A. Solution by Use of a Mathieu Equation

The applied magnetic field in the z direction is composed of a dc bias component H_B and a pump field $H_p \cos\omega_p t$. A change of variable will now be made from $\frac{\omega_p t}{2}$ to τ. Making this substitution equation 65 becomes

$$\ddot{\phi}(\tau) - \frac{2\alpha\gamma M}{\mu_o \omega_p}\dot{\phi}(\tau) + \frac{4\gamma^2 M}{\mu_o \omega_p^2}\left[\frac{2K}{M} + H_B + H_p \cos 2\tau\right]\phi(\tau)$$

$$= H_y(\tau)\left(\frac{4\gamma^2 M}{\omega_p^2 \mu_o}\right) \tag{66}$$

For simplicity equation 66 will be written as

$$\ddot{\phi} + 2A\dot{\phi} + (B + C\cos 2\tau)\phi = KH_y \tag{67}$$

where

$$A = -\frac{\alpha\gamma M}{\mu_o \omega_p}$$

$$B = \frac{4\gamma^2 M}{\mu_o \omega_p^2}\left(\frac{2K}{M} + H_B\right)$$

$$C = \frac{4\gamma^2 M H_p}{\mu_o \omega_p^2}$$

$$K = \frac{4\gamma^2 M}{\mu_o \omega_p^2} \tag{68}$$

To convert equation 67 to the form of a Mathieu equation let

$$\phi = ye^{-A\tau}$$

Making this substitution equation 67 becomes

$$\ddot{y} + \left[B - A^2 + C\cos 2\tau\right]y = KH_y(\tau)e^{A\tau} \tag{69}$$

Now let

$$a = B - A^2$$

$$-2q = C$$

Equation 69 then becomes

$$\ddot{y} + (a - 2q\cos 2\tau)y = KH_y(\tau)e^{A\tau} \tag{70}$$

Equation 70 is in the form of a Mathieu equation with a driving function. Considering the homogeneous part of equation 70 gives

$$\ddot{y} + (a - 2q\cos 2\tau)y = 0 \tag{71}$$

Equation 71 is a particular case of a linear type of equation of second order with a periodic coefficient. Its solutions take on different forms according to the values of a and q. The values of a and q also determine the stability

of the solution of the equation. Figure 2 is a graph of a versus q showing the regions of stable and unstable solutions. This graph, as described in detail by McLachlan (15) comes about by equating a to a function of q with a running index m. The curves themselves give values of a and q which result in periodic solutions of the homogeneous Mathieu equation and these solutions are called Mathieu functions of a certain order m. In between these curves lie the regions of stability or instability which give solutions of fractional order and are represented by a periodic type solution multiplied by a complex exponential. The most general type of solution of the second order equation considered is of the form

$$y(\tau) = Ae^{\mu\tau} \sum_{n=-\infty}^{\infty} C_n e^{jn\tau} + Be^{-\mu\tau} \sum_{n=-\infty}^{\infty} C_n e^{-jn\tau} \qquad (72)$$

where μ may be real, imaginary or complex. If the C_n's are considered to be complex, μ can be considered real or imaginary but not complex. The choice of whether μ is real or imaginary is determined by where on the stability chart the point a q lies. A and B in equation 72 are arbitrary constants determined by the initial conditions.

If equation 72 is substituted into equation 71 and coefficients of like terms in τ equated, the following recurrence results

Figure 2. Stability chart for the Mathieu equation $\ddot{y} + (a - 2q\cos 2\tau)y = 0$ (15, p. 40)

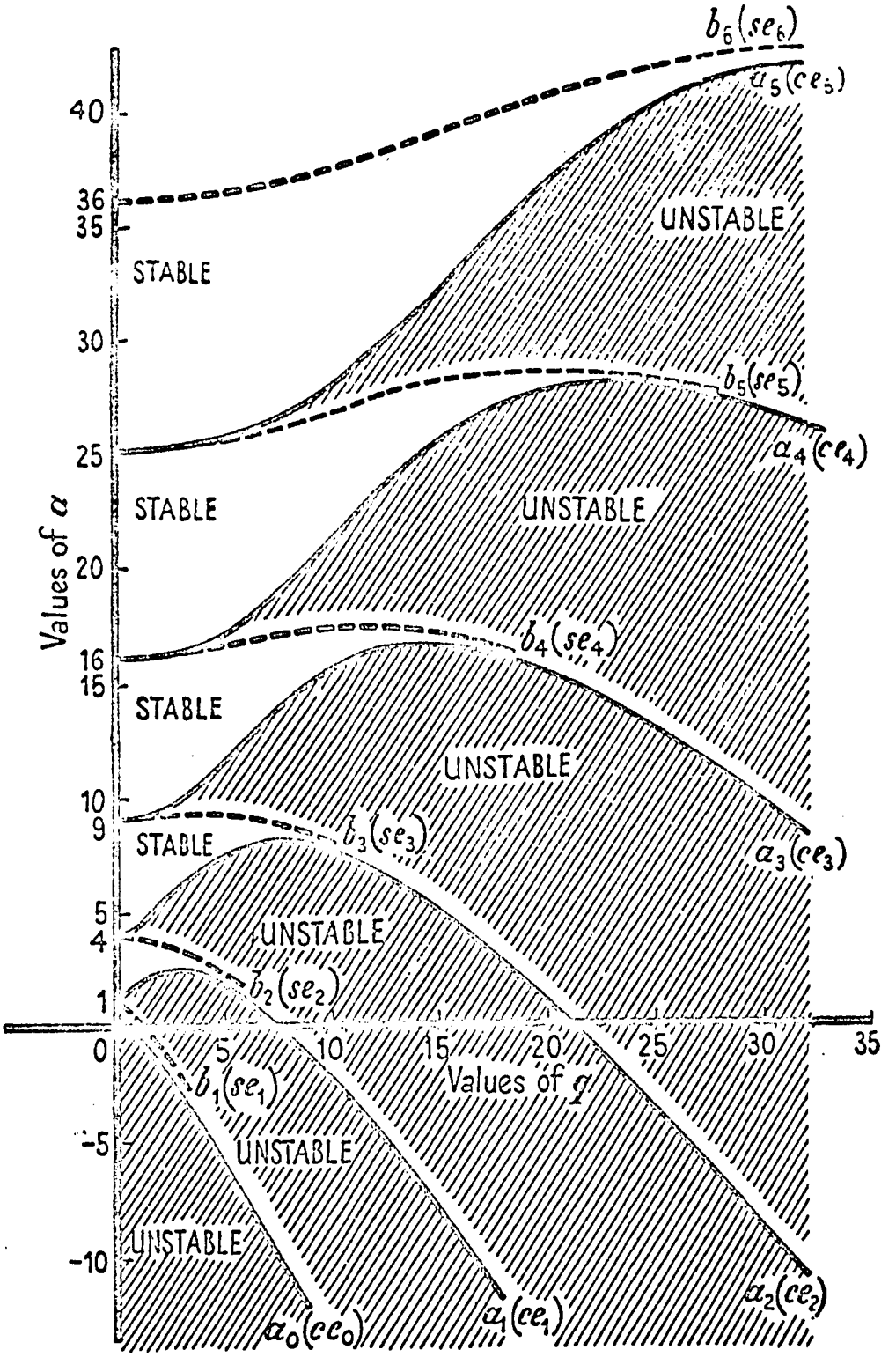
$b_6(se_6)$
$a_5(ce_5)$
UNSTABLE
STABLE
$b_5(se_5)$
$a_4(ce_4)$
UNSTABLE
STABLE
$b_4(se_4)$
UNSTABLE
STABLE
$b_3(se_3)$
$a_3(ce_3)$
UNSTABLE
STABLE
$b_2(se_2)$
$b_1(se_1)$
UNSTABLE
UNSTABLE
$a_0(ce_0)$
$a_1(ce_1)$
$a_2(ce_2)$
Values of a
Values of q
40
36
35
30
25
20
16
15
10
9
5
4
1
0
-5
-10
5
10
15
20
25
30
35

$$\left[a - (n + \beta)^2\right]C_n - q\,(C_{n+2} - C_{n-2}) = 0 \qquad (73)$$

If the functions are periodic in 2π, as the ones considered in this dissertation are, then n may be replaced by $2r + 1$. If the solutions lie in the stable regions of the stability chart then $\mu = j\beta$. Equation 72 then becomes

$$y(\tau) = A \sum_{r=-\infty}^{\infty} C_{2r+1} e^{j(2r+1+\beta)\tau} + B \sum_{r=-\infty}^{\infty} C_{2r+1} e^{-j(2r+1+\beta)\tau} \qquad (74)$$

Equation 74 represents then two linearly homogeneous solutions to equation 71. The two solutions are

$$y_1(\tau) = \sum_{r=-\infty}^{\infty} C_{2r+1} e^{j(2r+1+\beta)\tau}$$

$$y_2(\tau) = \sum_{r=-\infty}^{\infty} C_{2r+1} e^{-j(2r+1+\beta)\tau} \qquad (75)$$

It can be seen from equation 75 that $y_2(\tau) = y_1(-\tau)$.

Since equation 74 is the solution of equation 71 for the stable region $y(\tau) \to 0$ as $\tau \to \infty$. The solution of equation 70 for steady state conditions will be given by the particular

solution. To obtain the particular solution a variation of parameter method is used. This method is given in the Appendix.

The steady state solution of equation 70 is

$$y(\tau) = -\frac{y_1(\tau)}{W}\int^{\tau} y_2(u)F(u)du + \frac{y_2(\tau)}{W}\int^{\tau} y_1(u)F(u)du \tag{76}$$

where F(u) is the driving function. F(u) can be represented in the general form as

$$F(u) = e^{Au}\,(f_m e^{jmu} + f_m^* e^{-jm\mu}) \tag{77}$$

where m is the ratio of the frequency of the driving term divided by one half the pump frequency. There will be a solution $y_m(\tau)$ for every value of m considered and the total solution will be the sum of all the $y_m(\tau)$'s. Substituting equations 75 and 77 into 76 the result is

$$y_m(\tau) = \frac{1}{W}\Bigg[\sum_{r=-\infty}^{\infty} C_{2r+1}e^{-j(2r+1+\beta)\tau}$$

$$\int^{\tau}\sum_{r=-\infty}^{\infty} C_{2r+1}e^{\left[j(2r+1+\beta)+A\right]u}(f_m e^{jmu}+f_m^* e^{-jmu})du$$

$$- \sum_{r=-\infty}^{\infty} C_{2r+1} e^{j(2r+1+\beta)\tau} \int_{r=-\infty}^{\tau} \sum_{r=-\infty}^{\infty} e^{[-j(2r+1+\beta)+A]\mu}$$

$$(f_m e^{jmu} + f_m^* e^{-jm\mu})du \Big] \tag{78}$$

After performing the integration equation 78 becomes

$$y_m(\tau) = \frac{e^{[A-j(1+\beta)]\tau}}{W} \sum_{r=-\infty}^{\infty} C_{2r+1} e^{-j2r\tau} \sum_{r=-\infty}^{\infty} C_{2r+1}$$

$$\left(\frac{f_m e^{[A+j(2r+1+\beta+m)]\tau}}{A+j(m+2r+1+\beta)} + \frac{f_m^* e^{[A-j(m-2r-1-\beta)]\tau}}{A-j(m-2r-1-\beta)} \right)$$

$$- \frac{e^{[A+j(1+\beta)]\tau}}{W} \sum_{r=-\infty}^{\infty} C_{2r+1} e^{j2r\tau} \sum_{r=-\infty}^{\infty} C_{2r+1}$$

$$\left(f_m \frac{e^{[A+j(m-2r-1-\beta)]\tau}}{A+j(m-2r-1-\beta)} + \frac{f_m^* e^{[A-j(m+2r+1+\beta)]\tau}}{A-j(m+2r+1+\beta)} \right) \tag{79}$$

The solution can be transformed back in terms of ϕ by letting

$$\phi_m(\tau) = e^{-A\tau} y_m(\tau) \tag{80}$$

Equation 79 then becomes

$$\phi_m(\tau) = \frac{1}{W}\left[\sum_{r=-\infty}^{\infty} C_{2r+1}e^{-j2r\tau} \sum_{r=-\infty}^{\infty} C_{2r+1}\left(\frac{f_m e^{j(m+2r)\tau}}{A+j(m+2r+1+\beta)}\right.\right.$$

$$\left. + \frac{f_m^* e^{-j(m-2r)\tau}}{A-j(m-2r-1-\beta)}\right) - \sum_{r=-\infty}^{\infty} C_{2r+1}e^{j2r\tau} \sum_{r=-\infty}^{\infty} C_{2r+1}$$

$$\left.\left(\frac{f_m e^{j(m-2r)\tau}}{A+j(m-2r-1-\beta)} + \frac{f_m^* e^{-j(m+2r)\tau}}{A-j(m+2r+1+\beta)}\right)\right] \qquad (81)$$

It can be seen from the Appendix that W contains a product C_1^2. This product cancels out in equation 81 so that C_1 does not appear in the final solution. The magnitude of the remaining part of W will be denoted by W'.

The total solution will be the sum of all the ϕ_m's corresponding to the signal frequency ω_s, the difference frequency $\omega_p - \omega_s$, the sum or upper sideband frequency $\omega_p + \omega_s$, and all the higher order terms. The experimental amplifier, to be described later, was tuned to support the signal frequency and the difference frequency. The difference frequency is called the idler frequency. It can therefore be assumed that $\phi_m(\tau)$ is essentially made up of two terms ϕ_s and ϕ_i where ϕ_s corresponds to the signal frequency and ϕ_i represents the idler term.

The magnetic fields at the signal and idler frequencies

may be assumed to be of the form

$$h_m(\tau) = H_m \sin(m\tau + \varphi_m)$$

Therefore let

$$f_m = \frac{H_m}{2j} e^{j\varphi}$$

$$f_m^* = -\frac{H_m}{2j} e^{-j\varphi} \tag{82}$$

Making this substitution and also the substitution that $\tau = \frac{\omega t}{p}$ in equation 81 and simplifying saving only the terms corresponding to the signal and idler frequencies the result is

$$\phi_s(t) = \frac{KH_s}{W'} \left[A\cos(\omega_s t + \varphi_s) + B\cos(\omega_i t + \varphi_s)\right]$$

$$\phi_i(t) = \frac{KH_i}{W'} \left[B\cos(\omega_s t + \varphi_i) + C\cos(\omega_i t + \varphi_i)\right] \tag{83}$$

To find the equivalent voltages at the signal and idler frequencies multiply equation 83 by λ_m and differentiate with respect to time to obtain

$$\lambda_m \dot{\phi}_s(t) = -\frac{KH_s\lambda_m}{W'} \left[\omega_s A\sin(\omega_s t + \varphi_s) + \omega_i B\sin(\omega_i t + \varphi_s)\right]$$

$$\lambda_m \dot{\phi}_i(t) = -\frac{KH_i\lambda_m}{W'} \left[\omega_s B\sin(\omega_s t + \varphi_i) + \omega_i C\sin(\omega_i t + \varphi_i)\right] \tag{84}$$

If it is assumed that there exist some equivalent current I_{se} due to the magnetic field caused by the external signal source then

$$H_{se} = k_s I_{se} \tag{85}$$

where k_s depends on the signal structure of the parametric amplifier. Equation 84 can now be rewritten as

$$\lambda_m \dot{\phi}_s(t) = -\frac{k_s K \lambda_m}{W'}(I_{se} + I_{si})\left[\omega_s A\sin(\omega_s t+\varphi_s)+B\omega_i \sin(\omega_i t+\varphi_s)\right]$$

$$\lambda_m \dot{\phi}_i(t) = -\frac{k_i K \lambda_m}{W'} I_{is}\left[\omega_s B\sin(\omega_s t+\varphi_i) + C\omega_i \sin(\omega_i t+\varphi_i)\right] \tag{86}$$

where I_{si} equals the equivalent current at the signal frequency in the signal structure due to the idler and I_{is} equals the equivalent current at the idler frequency in the idler structure due to the signal. The total current in the signal structure is then $I_{se} + I_{si}$. The factor k_i is the constant retating the idler field to an equivalent current in the idler structure.

For the signal and idler structures tuned to resonance it can be assumed that there is no phase difference between the signal and idler.

The second term of the first equation of equation 86 is

the voltage generating the equivalent idler current I_{is}. Therefore let

$$V_{is} = - \frac{K(I_{se}+I_{si})}{W'} B\omega_i \lambda_m \tag{87}$$

The equivalent current I_{is} is equal to the voltage V_{is} divided by the equivalent impedance z_i of the idler structure. For a tuned structure z_i can be assumed to be a pure resistance R_i. Therefore let

$$I_{is} = - \frac{K(I_{se}+I_{si})}{W'R_i} B\omega_i \lambda_m \tag{88}$$

The current I_{si} is due to the voltage corresponding to the first term in the second equation of equation 86. A feedback voltage is thus generated at the signal frequency equal to $\frac{\lambda_m^2 K^2 k_s k_i \omega_s \omega_i}{W'^2 R_i} B^2(I_{se}+I_{si})$. If this voltage is divided by the equivalent current in the signal structure an equivalent negative resistance R is obtained which is

$$R = \frac{\omega_i \omega_s K^2 k_i k_s B^2 \lambda_m^2}{W'^2 R_i} \tag{89}$$

When the signal source is matched to the parametric amplifier the power input is $\frac{E_g^2}{4R_g}$ where E_g equals the voltage

of the signal generator and R_g equals the resistance of the signal generator. The output current from the amplifier assuming the parametric amplifier is matched to the load is

$$I = \frac{E_g}{[R_g+R_L+R_s-R]} \tag{90}$$

where R_L equals the load resistance and R_s is the equivalent resistance of the tuned signal structure of the parametric amplifier. The power out can be represented as

$$P_{out} = I^2 R_L = \frac{R_L E_g^2}{[R_g+R_L+R_S-R]^2} \tag{91}$$

The gain of the parametric amplifier can be calculated as

$$\text{Gain} = \frac{P_{out}}{P_{in}} = \frac{4R_L R_g}{[R_L+R_g+R_s-R]^2} \tag{92}$$

It can be seen that the threshold condition is when $R = R_s$ as the gain is then equal to one.

B. Solution by Use of an Equivalent Circuit

The general equation of motion for the magnetic material can be written as

$$\frac{\mu_o \ddot{\lambda}(t)}{\gamma^2 M \lambda_m} + \frac{\alpha \dot{\lambda}(t)}{\gamma \lambda_m} + (H_K+H_B+H_p \cos \omega_p t) \frac{\lambda(t)}{\lambda_m} = k_T i_T \tag{93}$$

where the transverse field is represented by a constant times an equivalent current. Also the substitution $\phi = \frac{\lambda}{m}$ has been made since

$$\lambda_m \sin\phi = \lambda \triangleq \lambda_m \phi \tag{94}$$

for the small signal case. Equation 93 then can be written as

$$C \frac{de}{dt} + \frac{1}{R} e + \frac{1}{L} \int e dt = i_T \tag{95}$$

where e has been substituted for $\dot{\lambda}$. This equation is a node voltage equation for a parallel LRC circuit. This representation gives

$$C = \frac{\mu_o}{\gamma^2 M \lambda_m k_T}$$

$$R = \frac{\gamma \lambda_m k_T}{\alpha}$$

$$L = \frac{\lambda_m k_T}{H_K + H_B + H_p \cos\omega_p t} \tag{96}$$

Figure 3A is an equivalent circuit for the magnetic material with equivalent idler and signal circuits attached. The impedances z_i and z_s are the total impedances of the idler and signal structures except for the part due directly to the magnetic material.

The inductance L may be expanded in an infinite series. This has been done by Read (21) and the result is

Figure 3A. Equivalent circuit for the parametric amplifier using a parallel RLC representation for the magnetic material

Figure 3B. A reduced equivalent circuit of the parametric amplifier

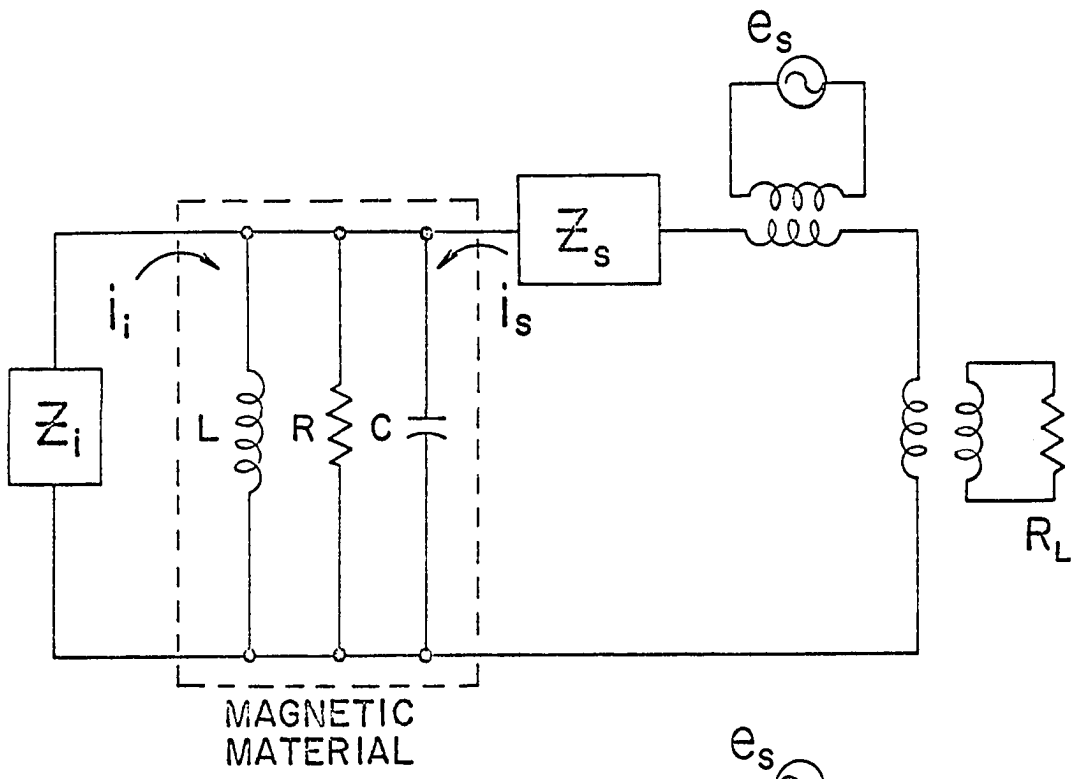
e_s
Z_s
i_i
i_s
Z_i
L
R
C
R_L
MAGNETIC
MATERIAL

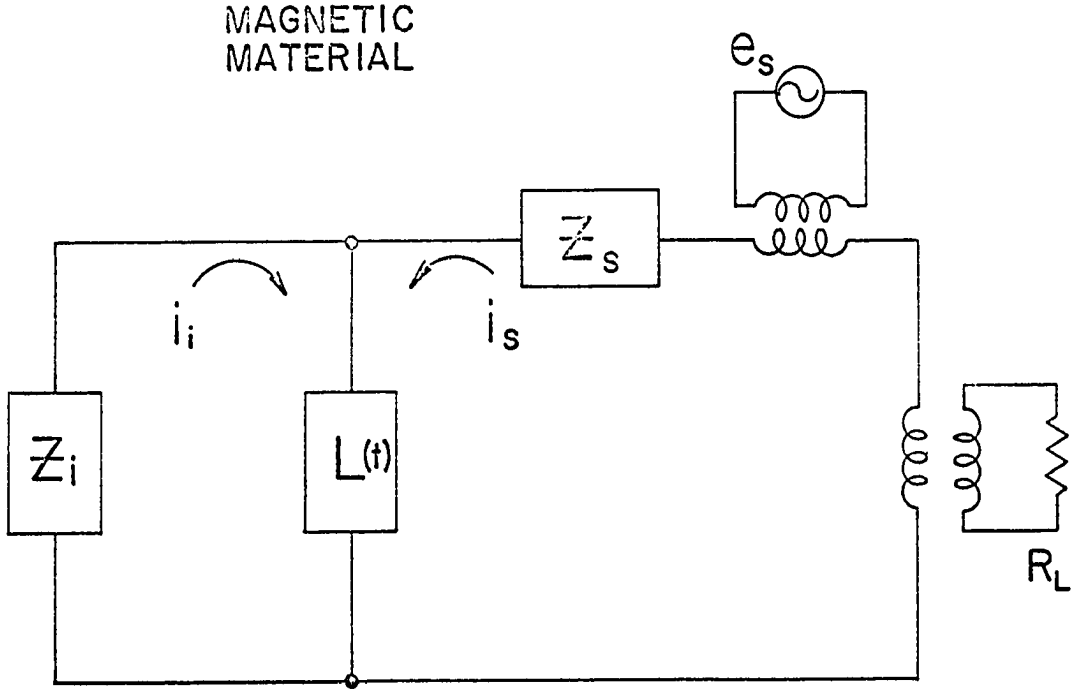
e_s
Z_s
i_i
i_s
Z_i
$L(t)$
R_L

$$L = \frac{L_o A_o}{2} + L_o \sum_{n=1}^{\infty} (-1)^n A_n \cos n\omega_p t \tag{97}$$

where

$$\gamma = \frac{H_p}{H_K + H_B}$$

$$L_o = \frac{\lambda_m k_T}{H_K + H_B}$$

$$A_n = \frac{2}{\sqrt{1-\gamma^2}} \left[\frac{1-\sqrt{1-\gamma^2}}{\gamma} \right]^n \tag{98}$$

A plot of the first six values of A_n as a function of the pumping parameter γ is shown in Figure 4. From Figure 4 it can be seen that, for small values of γ, A_n is equal to γ^n. It should be emphasized that equation 97 is valid only for small angles of rotation of the magnetization vector. Equation 97 is therefore an equation of a time-varying inductor but as far as the signal structure is concerned it is a linear element.

The non time-varying part of the inductance, capacitance, and resistance of the magnetic material can be considered a part of z_i and z_s. The circuit can now be represented as shown in Figure 3B. If the structure is resonated with the magnetic material present, the effects of the non time-varying part of the inductance and capacitance are tuned out and the

Figure 4. The coefficient of inductance A_n as a function of the pump amplitude parameter γ (20, p. 31)

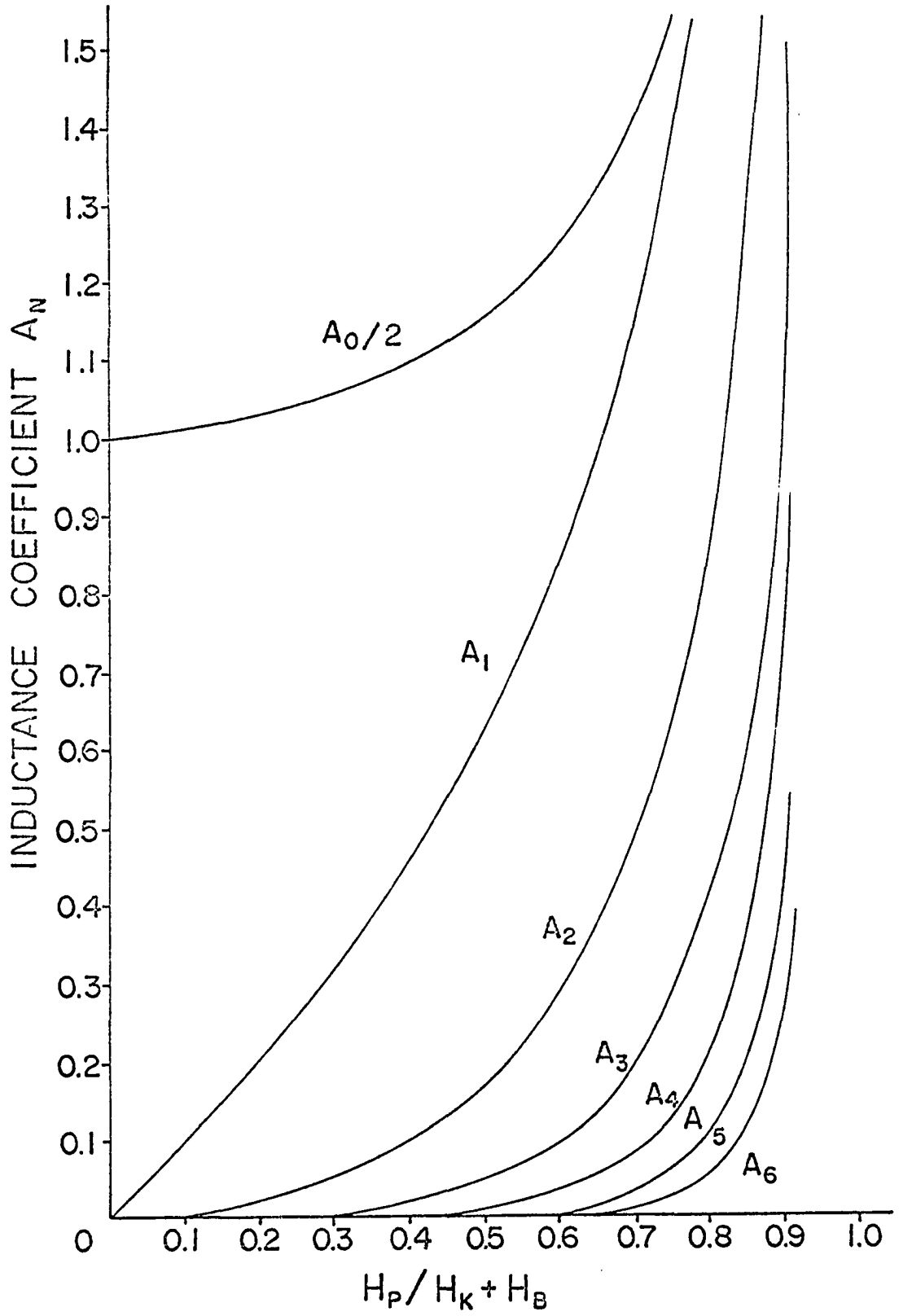
INDUCTANCE COEFFICIENT A_N
1.5
1.4
1.3
1.2
1.1
1.0
0.9
0.8
0.7
0.6
0.5
0.4
0.3
0.2
0.1
0
$A_0/2$
A_1
A_2
A_3
A_4
A_5
A_6
0.1
0.2
0.3
0.4
0.5
0.6
0.7
0.8
0.9
1.0
$H_P / H_K + H_B$

resistance is taken into account by the equivalent resistance of the tuned structure.

The equivalent current due to the magnetic fields in the signal structure can be represented as

$$i_s = \sum_{m=1}^{\infty} I_m \sin(\omega_m t + \varphi_m) \tag{99}$$

For a tuned structure it can be assumed that all fields are negligible in the signal structure except the field at the signal frequency. Equation 99 can then be written as

$$i_s = I_s \sin(\omega_s t + \varphi) \tag{100}$$

The flux linkage due to the film may be obtained by taking the product of $L(t)$ and i_s. The time derivative of this product gives the voltage across the signal and idler structures due to the time-varying part of the inductance of the magnetic material. This voltage can be expressed as

$$e_s = L_o \sum_{n=1}^{\infty} (-1)^n A_n \left(\frac{I_s}{2}\right) \left\{ (n\omega_p + \omega_s) \cos\left[(n\omega_p + \omega_s) t + \varphi \right] \right.$$

$$\left. + (n\omega_p - \omega_s) \cos\left[(n\omega_p - \omega_s) t - \varphi \right] \right\} \tag{101}$$

The parametric amplifier considered here is tuned to support the signal frequency ω_s and the idler frequency

$\omega_p - \omega_s = \omega_i$. Therefore it can be assumed that the field existing in the idler structure is due to the voltage at the difference frequency ω_i. This voltage is

$$e_i = - \frac{L_o A_1 I_s \omega_i}{2} \cos(\omega_i t - \psi) \tag{102}$$

The impedance of the idler structure can be represented as

$$Z_i = | Z_i | e^{j\theta} \tag{103}$$

Referring to Figure 3B it can be seen that

$$i_i = - \frac{e_i}{Z_i} = \frac{A_1 L_o I_s \omega_i}{2|Z_i|} \cos (\omega_i t - \psi - \theta) \tag{104}$$

The flux linkage due to the idler current can be found by taking the product of equation 104 and the time varying part of equation 97. The time derivative of this flux linkage creates a voltage which is impressed across the equivalent signal circuit. The voltage is

$$\frac{d\lambda_i}{dt} = \frac{L_o^2 A_1 \omega_i}{2|Z_i|} \sum_{n=1}^{\infty} (-1)^n A_n \frac{I_s}{2} \left\{ (n\omega_p + \omega_i) \sin \left[(n\omega_p + \omega_i) t - \psi - \theta \right] \right.$$

$$\left. + (n\omega_p - \omega_i) \sin \left[(n\omega_p - \omega_i) + \psi + \theta \right] \right\} \tag{105}$$

The term of equation 105 at the signal frequency produces a

current in the signal circuit. This component of voltage due to the idler is

$$e_{si} = - \frac{L_o^2 A_1^2 \omega_i \omega_s I_s}{4|Z_i|} \sin(\omega_s t + \phi + \theta) \tag{106}$$

This equation can be rewritten as

$$e_{si} = - \frac{L_o^2 A_1^2 \omega_i \omega_s I_s}{4Z_i^*} \sin(\omega_s t + \phi) \tag{107}$$

When the idler structure is tuned to resonance the impedance seen is pure resistive therefore $z_i = z_i^* = R_i$. If e_{si} is divided by the equivalent current of the signal structure an impedance term results which is an equivalent negative resistance -R. The value of this resistance is

$$-R = - \frac{\omega_s \omega_i L_o^2 A_1^2}{4R_i} \tag{108}$$

It can be seen that the expression for the negative resistance is very similar to equation 89 of part A. The same expression for gain will be used as given in equation 92.

IV. EXPERIMENTAL RESULTS

A. Harmonic Generator

Figure 5 shows a block diagram of the experimental model of the harmonic generator. For an input power above 6 watts it was necessary to replace the variable attenuator with a 1300 mc circulator terminated in 50 ohms on one terminal and a double-stub tuner to control the output power.

The harmonic generator is shown in Figure 6. The helmholtz coils were used to produce the dc bias field. The input power terminal is terminal A. The power is coupled into a resonant air line by a coupling loop. A short piece of stripline is attached to the center conductor of the resonant line and is grounded after going over the sample as shown in Figure 7. The stripline was about 75 mils wide and 2.5 mils thick.

The resonant air line with the magnetic sample in place and the dc bias applied was tuned to 1300 mc, the frequency of the incoming power.

The output structure was similar to the input structure with the output stripline about 37.5 mils wide. The output structure was resonated at twice the input frequency. The output resonant line, besides supporting the second harmonic component of magnetic field, also helped filter out any power fed through at the input frequency. The high pass filter

Figure 5. Block diagram of the second harmonic generator circuit

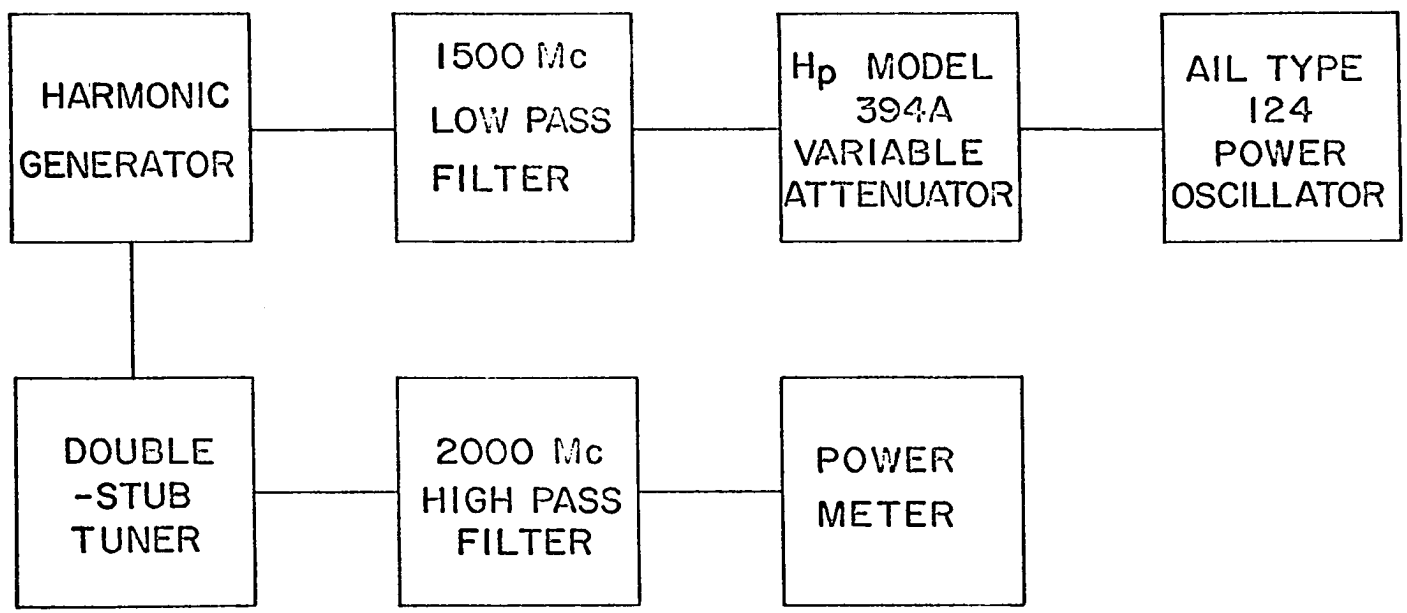
HARMONIC GENERATOR
1500 Mc LOW PASS FILTER
Hp MODEL 394A VARIABLE ATTENUATOR
AIL TYPE 124 POWER OSCILLATOR
DOUBLE -STUB TUNER
2000 Mc HIGH PASS FILTER
POWER METER

Figure 6. Harmonic generator

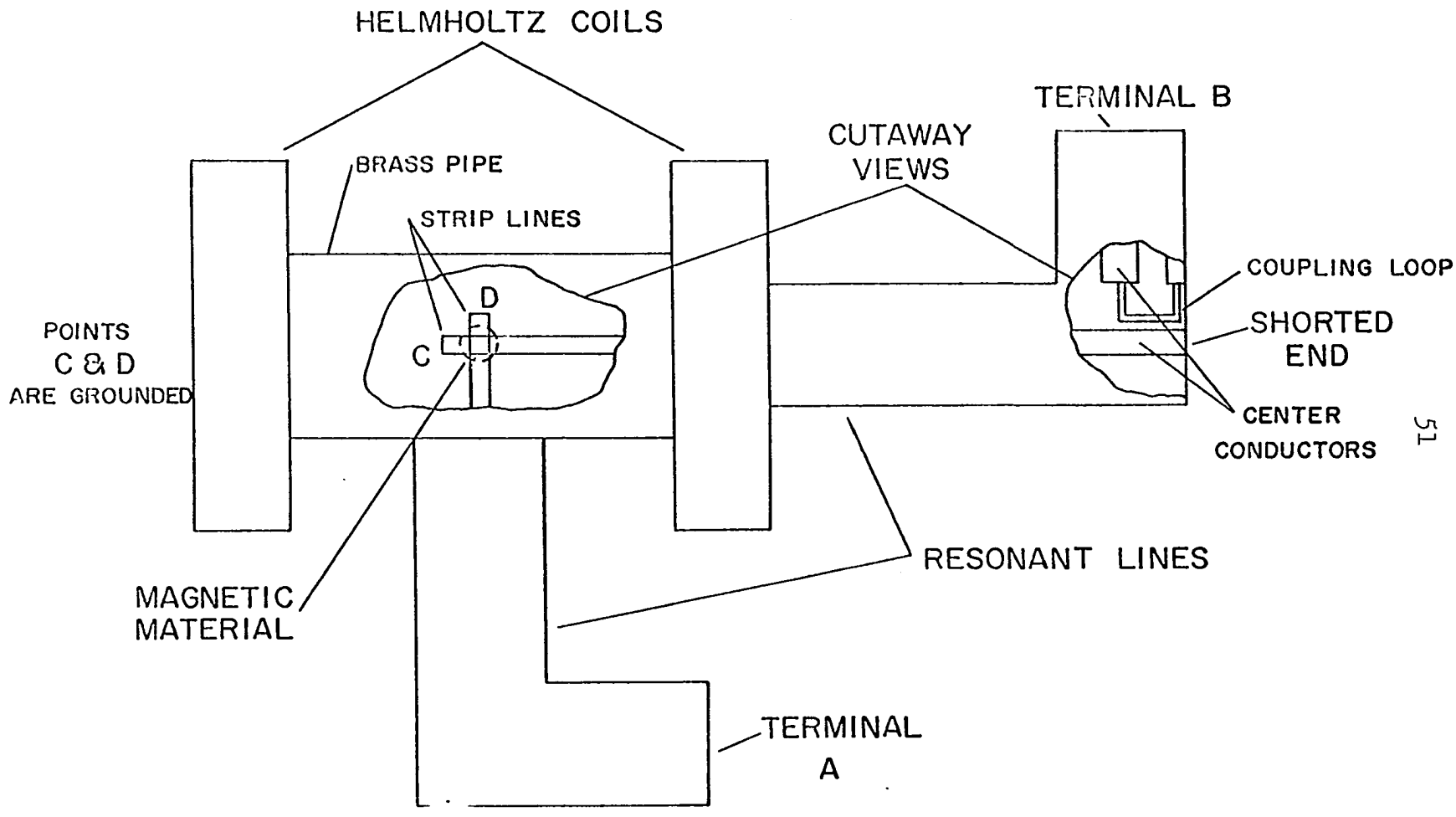
HELMHOLTZ COILS
TERMINAL B
CUTAWAY VIEWS
BRASS PIPE
STRIP LINES
COUPLING LOOP
SHORTED END
D
C
POINTS C & D ARE GROUNDED
CENTER CONDUCTORS
RESONANT LINES
MAGNETIC MATERIAL
TERMINAL A

Figure 7. Structure for coupling to the magnetic material in the harmonic generator

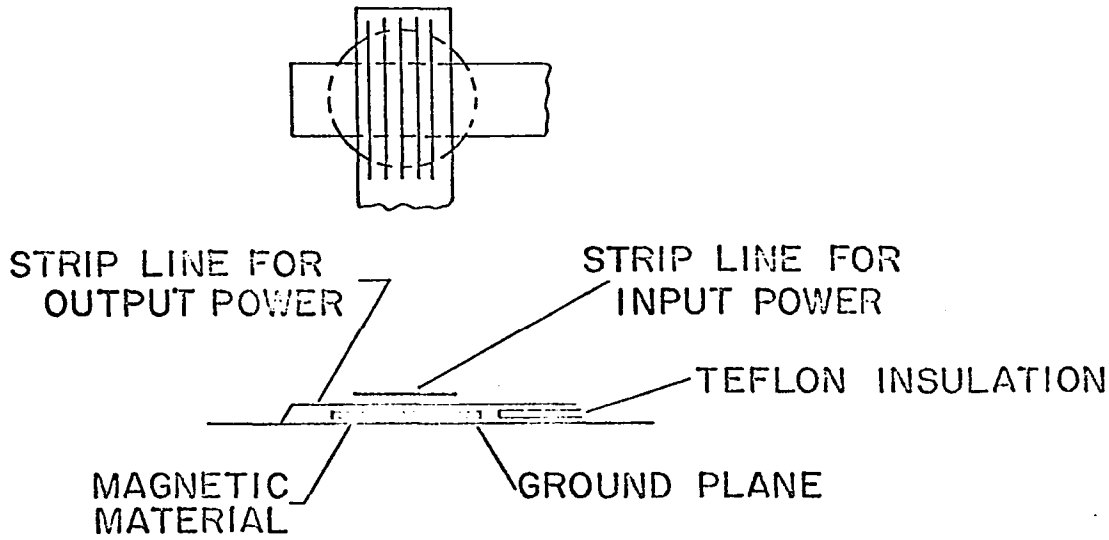
STRIP LINE FOR
OUTPUT POWER
STRIP LINE FOR
INPUT POWER
TEFLON INSULATION
MAGNETIC
MATERIAL
GROUND PLANE

acted to further attenuate any output signal at the input frequency. The double-stub tuner acted as a band-pass filter and its purpose was to filter out any of the higher order harmonics present in the output signal.

Both striplines were slit into fine strips where they crossed over the magnetic material. This was done to decrease eddy currents in the stripline and to decrease shielding effects of the stripline.

Figure 8 shows a graph of the output power as a function of the input power squared for a thin magnetic film harmonic generator. The film sample used was 1500 A^{o} thick and about 150 mils in diameter deposited on a six mil thick glass substrate. Except at low input power levels the results substantiated those predicted theoretically, that is

$$P_{out} = K P_{in}^{2} \tag{109}$$

The value of K was observed to be about 9×10^{-5}.

The experimental structure as shown in Figure 7 was found to be the most efficient. A two turn coil was substituted for the output stripline but it was necessary to space the turns about 10 mils apart and also to make the coil slightly rounding to raise its resonants frequency above the output frequency. The result was an apparent poorer coupling than for the stripline and the Q of the output resonant line dropped from 60 to 30. The output was down

Figure 8. Output power at the second harmonic versus the square of the input power for the harmonic generator using magnetic thin films

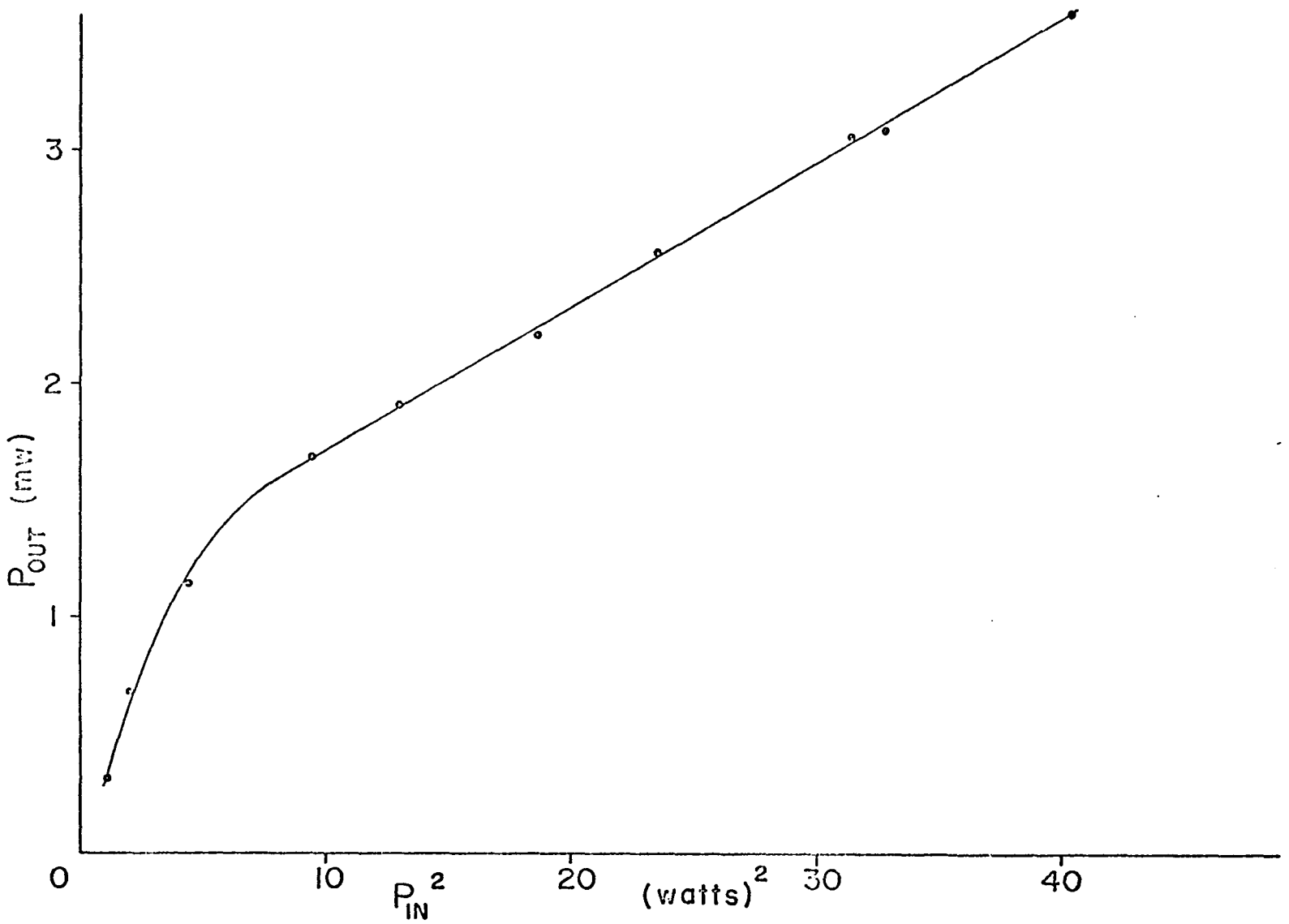
3
2
1
0
P_{OUT} (mw)
10
20
30
40
P_{IN}^2
(watts)^2

20 db more than the results in Figure 8.

When a YIG disk 5 mils thick and 150 mils in diameter was substituted for the thin magnetic film the resulting output was down about 8 db further than the equivalent output for the thin magnetic film. The graph of the output power versus the square of the input power was linear as for the thin magnetic film but the slope was slightly less.

The value of bias field for optimum output for the thin magnetic film was about 19 oersteds. Using equation 28 this bias corresponds to a resonant frequency of about 1300 mc. The optimum bias for the YIG disk was about 90 oersteds which also corresponded to a resonant frequency of 1300 mc. The values of M used in the calculations was $M = 10^4$ gauss for the thin magnetic film and M = 1750 gauss for the YIG disk. The values of H_K were measured to be about 2.75 oersteds for the thin magnetic film and 40 oersteds for the YIG disk.

Heating effects were also observed at the higher power levels for both the thin magnetic film and the YIG disk. If the power was left on for any length of time a decrease was observed in the output power. The magnetic thin film showed a greater change than the YIG disk and permanent damage resulted to the magnetic thin film when the power was left on for about 5 minutes at an input power level of 10 watts. No attempt was made to cool the magnetic material.

B. Parametric Amplifier

Figure 9 is a block diagram of the experimental circuit for the parametric amplifier. The pump power was controlled by the variable attenuator. When pump power above 6 watts was desired it was necessary to replace the variable attenuator with a circulator and a double-stub tuner as was done in the harmonic generator experiment.

The signal power at 400 mc was supplied by a HP Model 608C signal generator. The 500 mc low pass filter acted to block all frequencies except the signal frequency.

1. YIG parametric amplifier

The experimental structure for the parametric amplifier using a thin YIG disk is that shown in Figure 6 except the pump power was supplied at terminal A. The stripline in the pump structure was 150 mils wide and 6 mils thick. The purpose of the heavier stripline was to create a better heat sink for the YIG disk. The stripline was slit into thin strips to cut down eddy current losses and to allow the magnetic fields to penetrate. The pump structure was tuned to resonate at 1300 mc.

The signal power was supplied at terminal B. The stripline of the signal structure was replaced by 4 turns of No. 22 wire. This change was made to improve the coupling to the magnetic material although the resulting reduction in the Q

Figure 9. Block diagram of the parametric amplifier circuit

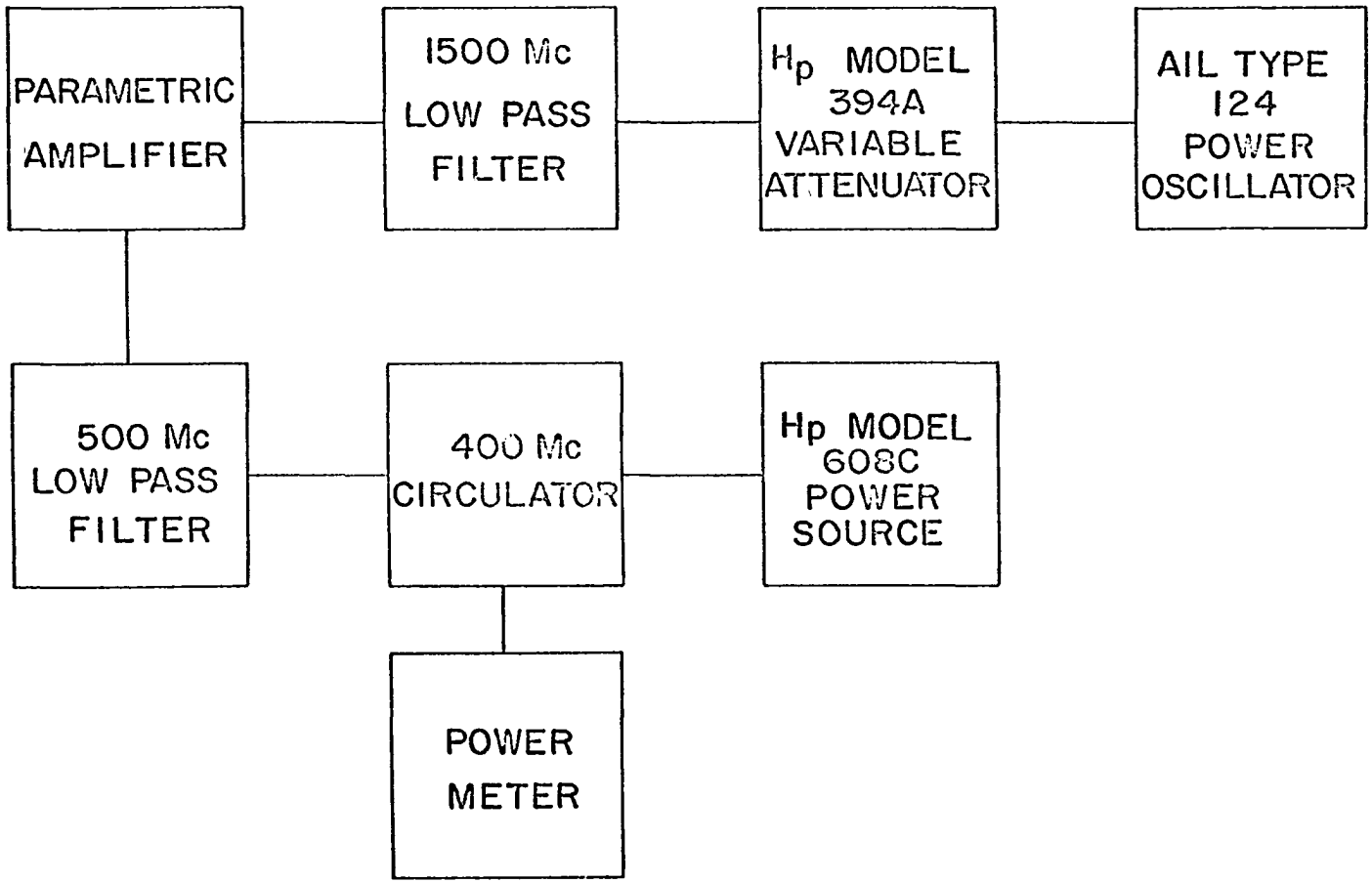
PARAMETRIC AMPLIFIER
1500 Mc LOW PASS FILTER
Hp MODEL 394A VARIABLE ATTENUATOR
AIL TYPE 124 POWER OSCILLATOR
500 Mc LOW PASS FILTER
400 Mc CIRCULATOR
Hp MODEL 608C POWER SOURCE
POWER METER

of the structure almost offset the gain in coupling. The signal structure was tuned to resonate at both 400 and 900 mc to support the signal and also the idler.

The YIG disk was oriented such that its easy axis was parallel to the bias and pump fields. The signal field was therefore applied perpendicular to the easy axis of magnetization.

The bias field was supplied to the magnetic material by helmholtz coils as shown in Figure 6. Theoretical analysis indicates that biasing for resonance at the signal frequency gives maximum output. It was not possible to resonate the YIG disk at 400 mc as the natural resonant frequency due to the anisotropy field was about 750 mc.

The parametric amplifier was analyzed for two different bias fields. At a value of bias of 7200 ampere turns per meter a slight increased in output over neighboring values of bias was observed. This bias corresponds to resonance at pump frequency. An optimum value of pump power for this value of bias was about 1.5 watts. This power corresponds to a pump field of approximately 1088 ampere turns per meter. Increasing the pump power caused the output first to decrease slightly and then to remain constant. Figure 10 shows a plot of the input signal power versus the output signal power. The input signal power recorded is that measured when the amplifier was replaced by a short. The gain for this value

Figure 10. Power out versus power in for the YIG parametric amplifier biased at pump resonance

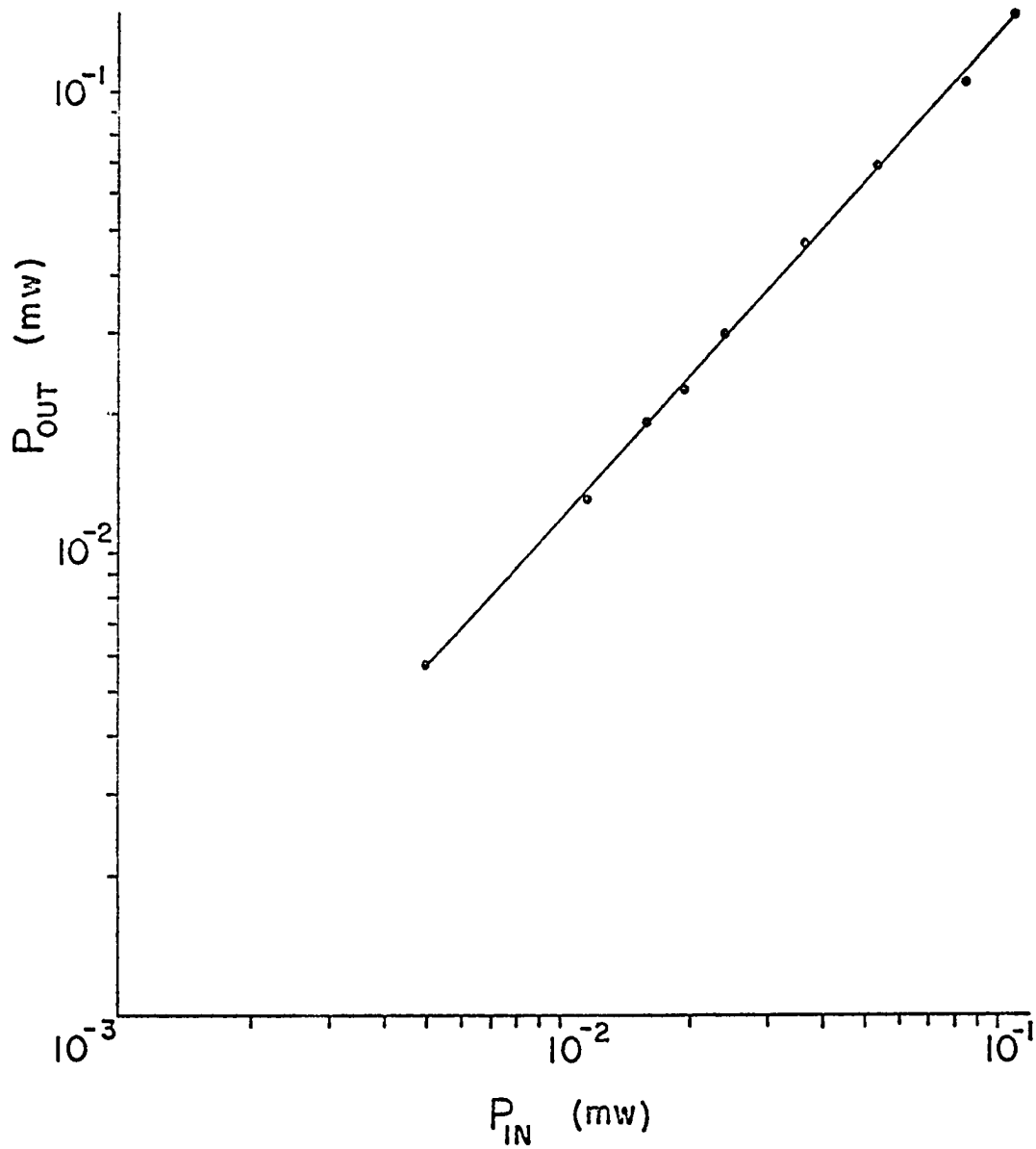
10^{-1}
10^{-2}
10^{-3}
P_{OUT} (mw)
10^{-2}
10^{-1}
P_{IN} (mw)

of bias was about 1 db.

For the signal power available no saturation effects were observed.

The Q of the signal structure was measured to be about 30 and the idler Q also was about 30. The effective loaded Q of the pump structure was about 50. The effective bandwidth was observed to be about 2 mc.

To calculate gain by use of the Mathieu equation the following constants were computed as

$$a = 4.25$$

$$q = 0.223$$

$$K = 4.1 \times 10^{-4}$$

$$A = 0.03775$$

The Mathieu equation becomes

$$\ddot{y} + (4.25 - 0.446\cos 2\tau)y = 4.1 \times 10^{-4} h_y e^{+0.03775\tau} \qquad (110)$$

For these values of a and q it can be seen from Figure 2 that the solutions lie in the stable region between a_2 and b_3.

It is observed that $\frac{a}{q} >> 1$ and q is quite small. Therefore, according to McLachlan (15), β will be approximately equal to $\sqrt{a}$ - m where m is the integral part of the square root of a. β is found to be equal approximately to 0.06. This value of β was used as a first approximation and was

checked in the recurrence relation. In the recurrence relation the values of C_{-11} and C_{11} were neglected with respect to C_{-9} and C_9 respectively. Using these approximations it was possible to obtain all the C_{2r+1}'s in terms of C_1. For a value of r = 0 the value of β was checked and found to give fair agreement considering slide rule accuracy.

The values of the C_{2r+1}'s from r = -5 to +4 were calculated and $y_1(\tau)$ was found to be

$$y_1(\tau) = C_1 \left[5.75\text{x}10^{-10}\, e^{-j8.94\tau} - 1.953\text{x}10^{-7}\, e^{-j6.94\tau} \right.$$

$$+ 3.85\text{x}10^{-5}\, e^{-j4.94\tau} - 3.34\text{x}10^{-3}\, e^{-j2.94\tau} + 6.6\text{x}10^{-2} e^{-j0.94\tau}$$

$$+ e^{j1.06\tau} - 4.365\text{x}10^{-2} e^{j3.06\tau} + 4.51\text{x}10^{-4} e^{j5.06\tau}$$

$$\left. - 2.235\text{x}10^{-6} e^{j7.06\tau} + 6.1\text{x}10^{-9} e^{j9.06\tau} \right] \qquad (111)$$

The value of $y_2(\tau)$ was obtained by letting $\tau = -\tau$ in $y_1(\tau)$. Only the terms from r = -2 to r = 2 were considered and these values of C_{2r+1}'s were substituted into equation 81. The value of A was much less than unity and was neglected in reducing equation 81. The magnitude of W was found to be 2.12.

The resulting equation in $\phi_m(\tau)$ is

$$\phi_m(\tau) = -k_m I_m \left(\frac{4.1\times10^{-4}}{2.12} \right) \left[2.67 \sin(m\tau + \psi_m) \right.$$

$$\left. + 0.1033 \sin \left\{(m-2)\tau + \psi_m\right\} \right] \qquad (112)$$

The values of m corresponding to the signal and the idler frequencies were substituted into equation 112. The equations were then converted to equations in time and differentiated with respect to time and multiplied by λ_m. The resulting equations are

$$\lambda_m \dot{\phi}_s = - \frac{\lambda_m k_s I_s (4.1\times10^{-4})}{2.12} \left[2.86\, \omega_s \cos(\omega_s t + \psi_s) \right.$$

$$\left. + 0.1033 \omega_i \cos(\omega_i t + \psi_s) \right]$$

$$\lambda_m \dot{\phi}_i = - \frac{\lambda_m k_i I_i (4.1\times10^{-4})}{2.12} \left[0.1033 \omega_s \cos(\omega_s t + \psi_i) \right.$$

$$\left. + 2.67 \omega_i \cos(\omega_i t + \psi_i) \right] \qquad (113)$$

The value of the equivalent negative resistance was then calculated using equation 89. The values of k_s and k_i were estimated to be approximately 10^3. The coupling between the YIG disk and the signal coil was estimated to be approximately 1/2. This small value was due to the loose

fitting of the coil about the YIG disk made necessary in order to slide the YIG disk and pump stripline in and out. The value of λ_m was then calculated to be approximately 1.355×10^{-7} webers per second.

The value of R_s and R_i were calculated using a method given by Ramo and Whinnery (19) concerning resonant lines. The value of a particular R_m is given as

$$R_m = \frac{L_m \omega_m}{Q_m} \tag{114}$$

where Q_m is the quality factor of the resonant line at a frequency corresponding to ω_m. L_m for a resonant air line is given as

$$L_m = \frac{lL}{2} \tag{115}$$

where l is the length of the resonant line and L is the inductance per unit length down the line. For an air line

$$L = \frac{\mu_o}{2\pi} \ln \frac{r_2}{r_1} \tag{116}$$

where r_2 equals the inside radius of the outside conductor and r_1 equals the outside radius of the inside conductor.

The values of Q_s and Q_i were measured to be both equal to 30. The values of R_i and R_s were calculated to both be

2.51 ohms. The value of the negative resistance was found to be about 41.5 ohms. The gain was calculated to be 2.68 or in db to be 4.28 db.

The value of gain was also calculated using the equivalent circuit method. The ratio of H_p to $H_B + H_K$ was about 0.1. From Figure 4 it can be seen that A_1 is equal to γ. The negative resistance was calculated to be 2.68 ohms. The value of gain was found to be approximately unity.

For the other recorded data the value of the bias field was increased to about 16,000 ampere turns per meter. One result was an increase in the idler Q from 30 to 40. The value of signal and pump Q remained essentially the same. Also increasing the bias made it possible to utilize more pump power. In fact, the pump power was increased up to 12 watts and the output was still going up slightly. A graph of the output power as a function of the input signal power is shown in Figure 11. The gain was fairly constant for the values of signal power considered here and was equal to about 1.2 db.

The value of the pump field corresponding to an input pump power of 12 watts was about 3345 ampere turns per meter. The Mathieu equation for these values of pump and bias fields is

$$\ddot{y} + (7.85 - 1.37 \cos 2\tau)y = Kh_y e^{+A\tau} \qquad (117)$$

Figure 11. Power out versus power in for the YIG parametric amplifier with 7200 ampere turns per meter bias

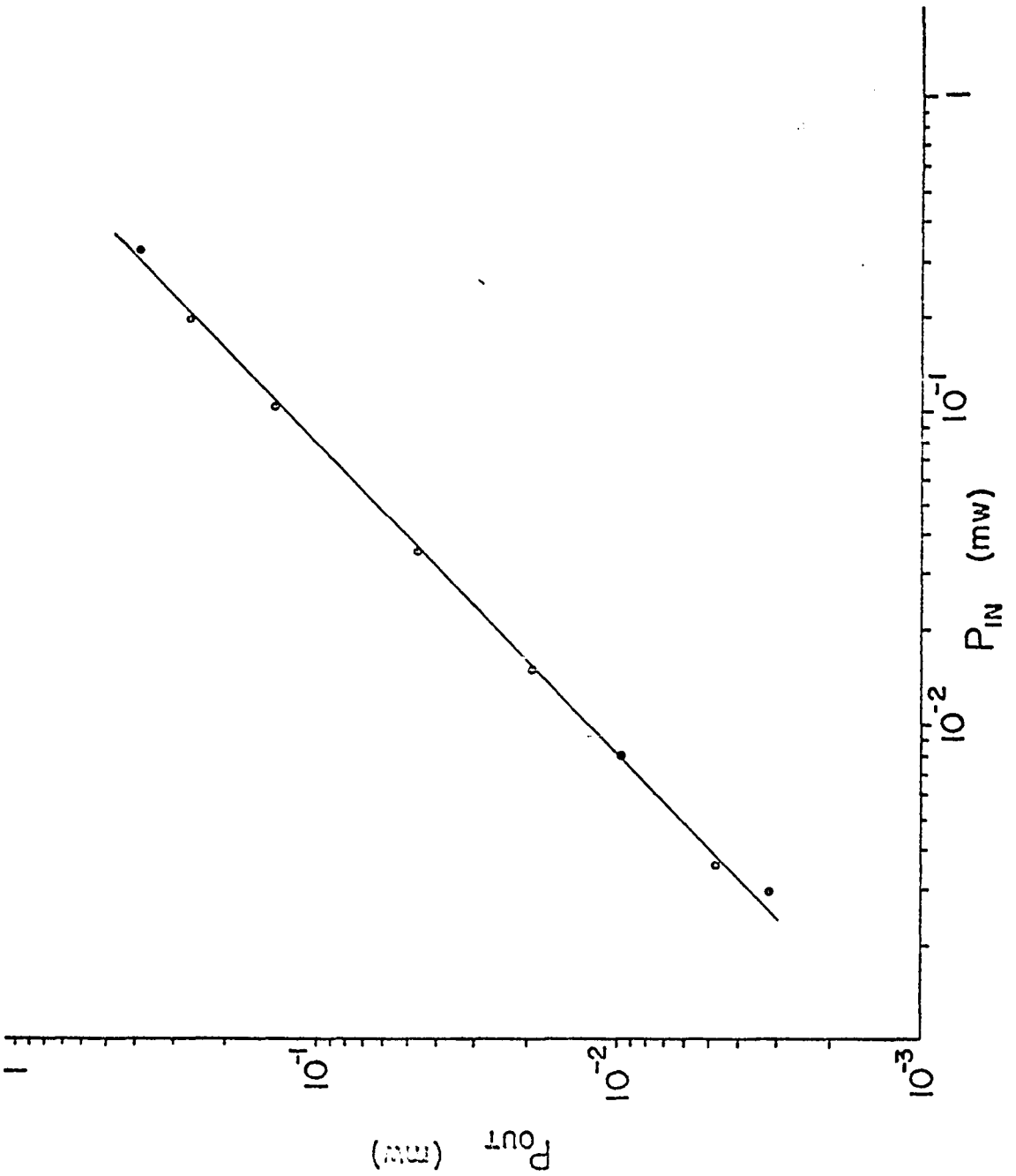
1
10^{-1}
10^{-2}
10^{-3}
P_{OUT} (mw)
1
10^{-1}
10^{-2}
P_{IN} (mw)

The solutions to equation 117 were found to lie in the same stable region as for the case just considered. The values of β and the C_{2r+1}'s were found the same way except it required several adjustments to arrive at a suitable value of β. A value of $\beta = 0.796$ was selected. The values of the C_{2r+1}'s were calculated using the recurrence relationship of equation 73. The value of $y_1(\tau)$ obtained is

$$y_1(\tau) = C_1 \left[-2.95\text{x}10^{-7} e^{-j8.204\tau} + 2.55\text{x}10^{-5} e^{-j6.204\tau} \right.$$

$$- 1.145\text{x}10^{-3} e^{-j4.204\tau} + 1.64\text{x}10^{-2} e^{-j2.204\tau}$$

$$+ 8.92\text{x}10^{-2} e^{-j0.204\tau} + e^{j1.796\tau} - 0.1049 e^{j3.796\tau}$$

$$+ 2.79\text{x}10^{-3} e^{j5.796\tau} - 3.612\text{x}10^{-5} e^{j7.796\tau}$$

$$\left. + 2.808\text{x}10^{-7} e^{j9.796\tau} \right] \qquad (118)$$

$Y_2(\tau)$ was set equal to $y_1(-\tau)$. $y_1(\tau)$ and $Y_2(\tau)$ were substituted into equation 81. Only the values of C_{2r+1}'s corresponding to r = -2 to r = 1 were considered in the calculations. The same procedure was followed as outlined in the previous case with the result

$$\lambda_m \dot{\phi}_s(t) = - \frac{KH_s\lambda_m}{3.674} \left[1.2755\, \omega_s \cos(\omega_s t + \psi_s) \right.$$

$$\left. + 0.2133\omega_i \cos(\omega_i t + \psi_s) \right]$$

$$\lambda_m \dot{\phi}_s(t) = - \frac{KH_i\lambda_m}{3.674} \left[0.2133\, \omega_s \cos(\omega_s t + \psi_i) \right.$$

$$\left. + 2.136\omega_i \cos(\omega_i t + \psi_i) \right] \qquad (119)$$

The resulting value of negative resistance was R = 77.2 ohms. The corresponding gain was 16.35 or 12 db.

For the equivalent circuit model the value of H_p over $H_B + H_K$ was again small so that $A_1 = \gamma$. Except for the pump and bias fields and R_i the other values were the same as in the previous case. The value of idler resistance R_i was calculated to be 1.91 ohms. The negative resistance was equal to about 2.81 ohms. The corresponding gain was found to be 1.02 or 0.2 db.

2. Magnetic thin film parametric amplifier

The parametric amplifier structure is shown in Figure 12. A 2000 A^o thick film pair about .8 cm long and about 0.1 cm wide is sandwiched on a 2.5 mil thick stripline. The easy axis of the film is perpendicular to the long dimension of

Figure 12. Magnetic thin film parametric amplifier

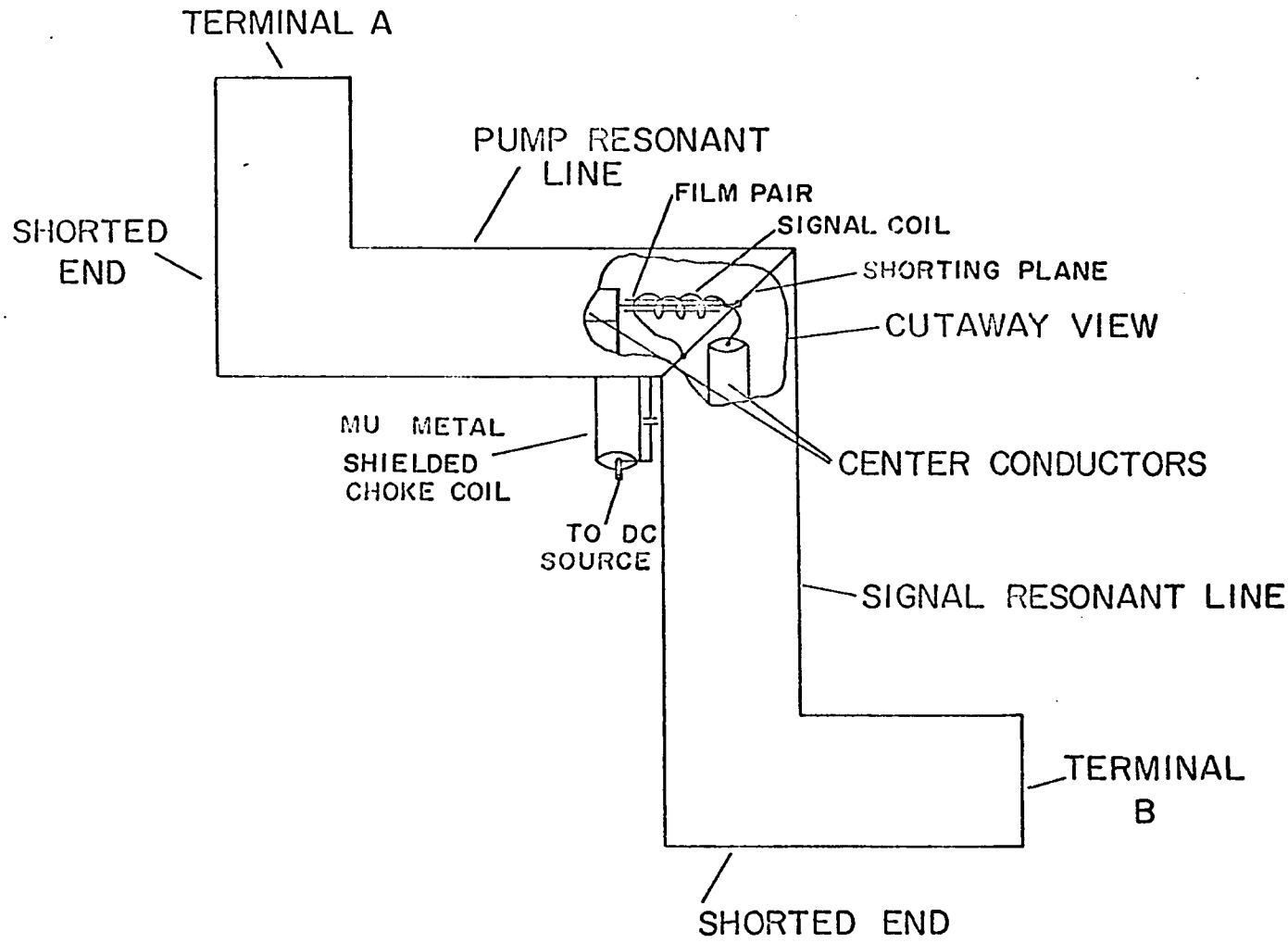
TERMINAL A
PUMP RESONANT LINE
FILM PAIR
SIGNAL COIL
SHORTED END
SHORTING PLANE
CUTAWAY VIEW
MU METAL SHIELDED CHOKE COIL
CENTER CONDUCTORS
TO DC SOURCE
SIGNAL RESONANT LINE
TERMINAL B
SHORTED END

the film. Ten turns of No. 28 wire was wrapped tightly about the film pair and the whole arrangement was set in epoxy. The one end of the stripline was fastened to the diagonal shorting plane between the pump and signal lines while the other end was connected to the center line of the pump resonant line.

The bias arrangement was connected as shown in Figure 12. A shielded choke coil and a capacitor were connected to the bias line where it left the pump resonant line to prevent loss of pump power. The coil shield, made of Mu metal, helped prevent the dc field in the choke coil from influencing the film pair. One end of the signal coil was connected through a hole in the shorting plane to the center conductor of the signal resonant line. The other end of the coil was attached to the shorting plane.

The amplifier was tuned to operate in the degenerate mode, that is, the pump frequency was equal to twice the signal frequency. The idler and signal frequencies are then the same. The pump frequency was 800 mc and the pump line was tuned to resonate at this value of frequency. The signal line was tuned to resonate at 400 mc.

The energy was coupled to the resonant lines by means of coupling loops as described in the harmonic generator.

The effective Q of the pump resonant line was about 15 while the Q of the signal line was about 30. The optimum

value of pump power was about 1 watt which corresponded to a pump field of about 1060 ampere turns per meter. Heating effects were observed at higher values of pump power.

The film pair was biased at about 875 ampere turns per meter. This bias corresponded to about the optimum value. At lower values of bias the pump field exceeded the bias plus anisotropy field. The result was a large loss of power in the amplifier. The value of bias plus anisotropy field was about 1075 ampere turns per meter which is about the same as the pump field.

The graph of the output power as a function of the input power is shown in Figure 13. The gain was essentially unity over the range of signal power considered. The difference between signal power out with pump on and then with pump off was about .5 db and this difference was also about constant over the range of signal power considered.

The Mathieu equation corresponding to the magnetic thin film parametric amplifier is

$$\ddot{y} + (6.34 - 6.52 \cos 2\tau)y = Kh_y(\tau)e^{0.525\tau} \qquad (120)$$

The value of q is larger than unity and the ratio of a to q is not $>>1$. To obtain a solution by this method it would be necessary to include in $y_1(\tau)$ at least about 11 terms as the values of the C_{2r+1}'s do not decrease rapidly as r is made

Figure 13. Power out versus power in for the magnetic thin film parametric amplifier

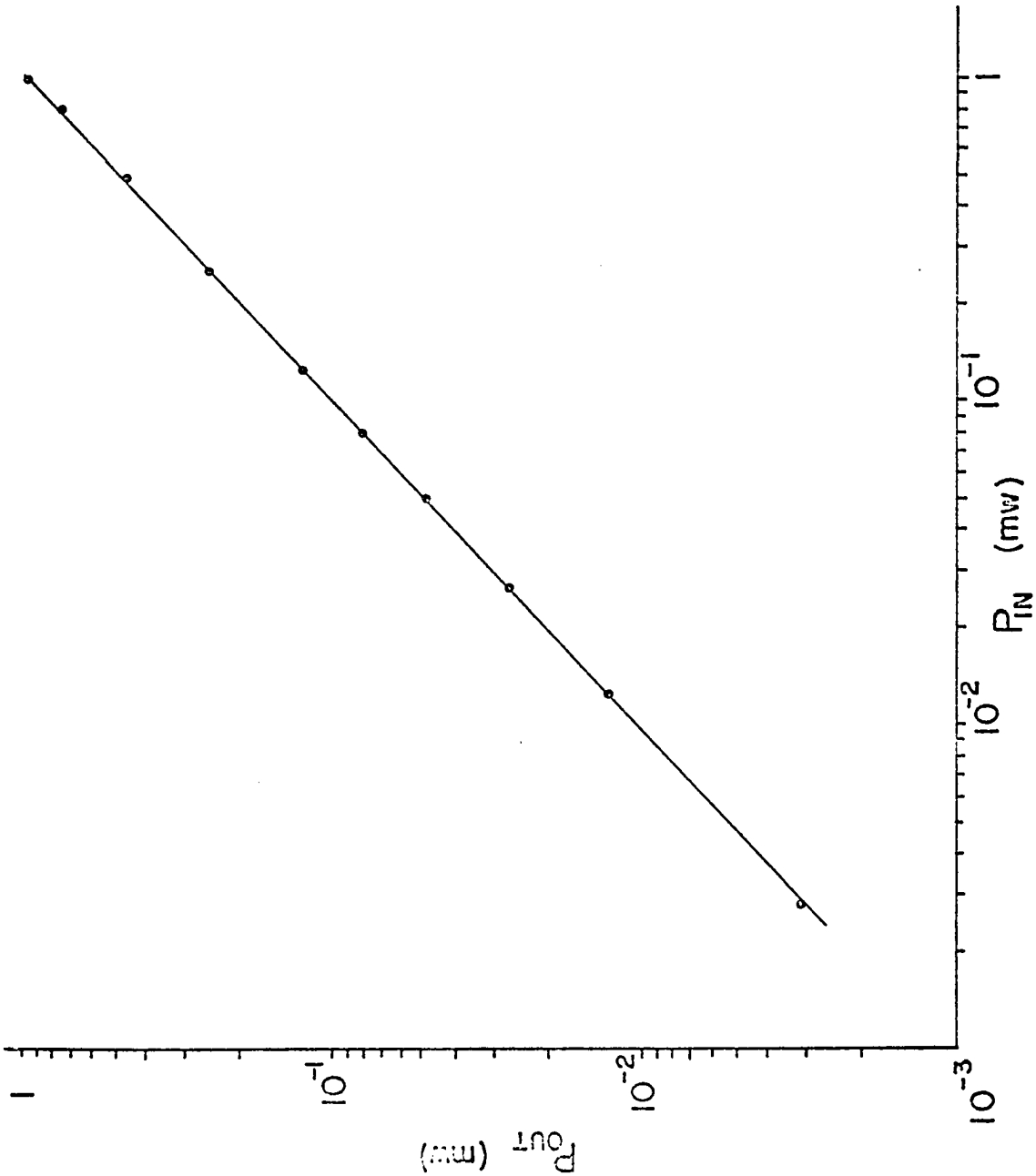
1
10^{-1}
10^{-2}
10^{-3}
P_{OUT} (mw)
10^{-2}
10^{-1}
1
P_{IN} (mW)

large either positive or negative. In substituting into equation 81 there is over 400 terms possible making manual calculation of a solution impractical.

The ratio of H_p to $H_B + H_K$ was essentially unity. The corresponding γ is then 1 making the value of A_1 infinite. The equivalent circuit method is no longer valid.

To obtain an analytic solution the Cyclone Computer was programmed to solve the general equation of motion for the magnetic thin film parametric amplifier by using a Runga Cutta method of solution. The equation of motion was written as

$$\ddot{\phi}(x) + a\dot{\phi}(x) + (b + d \cos 2x)\phi(x) = \sin(x + \varphi) \qquad (121)$$

where $x = \frac{\omega_p t}{2}$. The solutions for ϕ and $\dot{\phi}$ are shown plotted in Figure 14. Solutions were obtained for $\varphi = -\frac{\pi}{4}, 0, \frac{\pi}{4}$ and $\frac{\pi}{2}$. The values of ϕ and $\dot{\phi}$ were not significantly different but the largest values were observed when $\varphi = 0$ and $\frac{\pi}{4}$. A Fourier series analysis was then obtained for $\dot{\phi}$ through the use of the Cyclone Computer. The results are for $\varphi = \frac{\pi}{4}$

$$\phi(x) = 0.19274 \cos x - 0.0031 \sin x + 0.2351 \cos 3x$$

$$- 0.3704 \sin 3x + 0.0901 \cos 5x - 0.1200 \sin 5x + \cdots + \qquad (122)$$

Figure 14. Plot of ϕ and $\dot{\phi}$ from the solution by the Cyclone Computer of the equation of motion for the magnetic thin film parametric amplifier

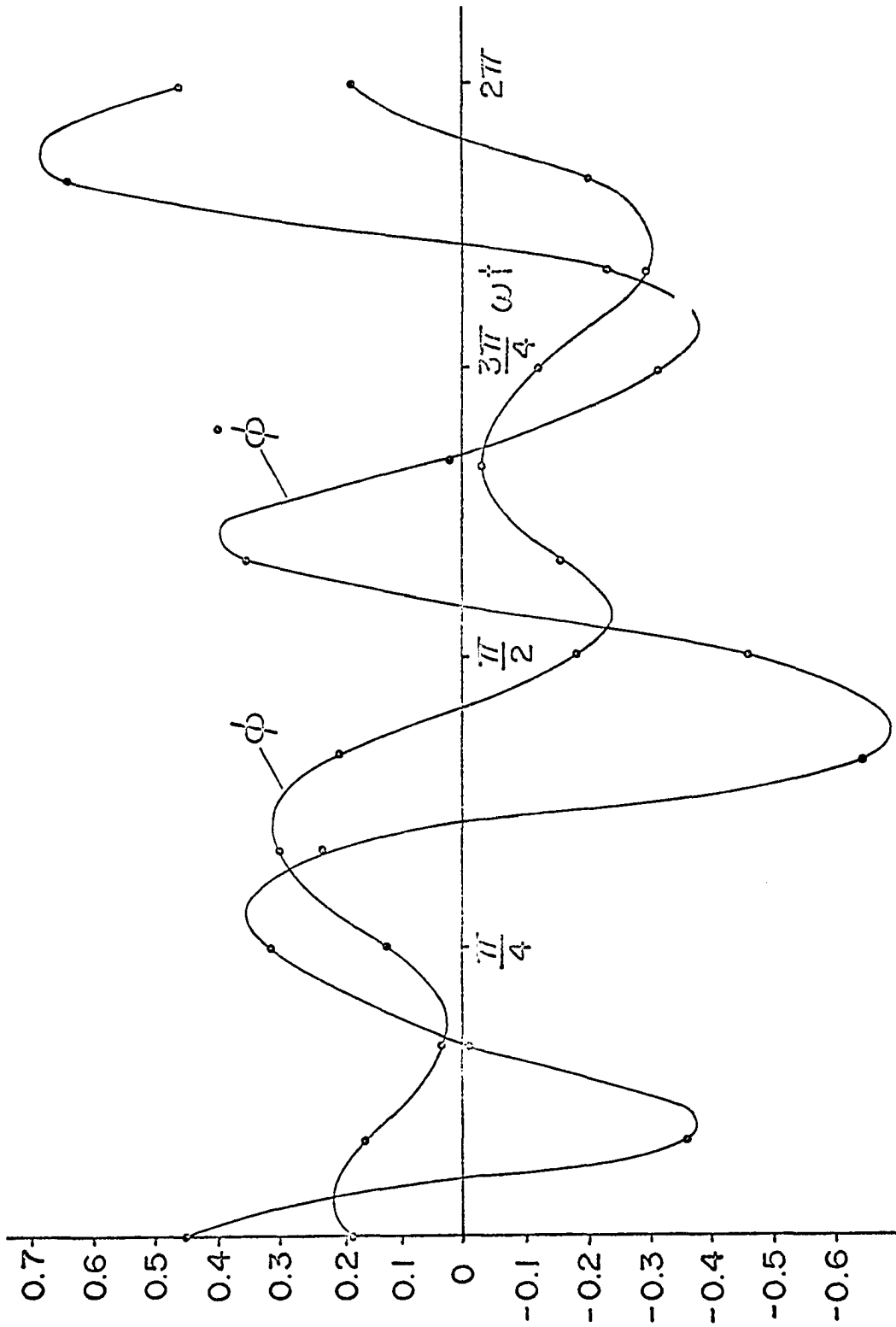
0.7
0.6
0.5
0.4
0.3
0.2
0.1
0
-0.1
-0.2
-0.3
-0.4
-0.5
-0.6
π/4
π/2
3π/4
ωt
2π
φ
φ̇

for $\psi = 0$

$$\dot{\phi}(x) = 0.2031 \cos x + 0.0695 \sin x + 0.4123 \cos 3x$$

$$-0.3704 \sin 3x + 0.0901 \cos 5x - 0.1200 \sin 5x + \cdots + \qquad (123)$$

To relate $\dot{\phi}(x)$ back to the actual problem it is necessary to convert from x to $\omega_s t$ and also to multiply by the coefficient of the driving function. All terms except the one at ω_s were neglected due to the signal structure being tuned to ω_s and also the signal structure was not resonant at $2\omega_s$ or higher multiples. The next higher resonant frequency was found to be at about 900 mc. For $\psi = \frac{\pi}{4}$ the solution becomes

$$\lambda_m \dot{\phi}(t) = K k_s \lambda_m I_s \omega_s \, 0.1927 \sin \omega_s t \qquad (124)$$

The value of k_s was calculated to be approximately 2000. λ_m was calculated using a coupling factor of 0.8 and was found equal approximately to 3×10^{-9} webers per second. K was equal to 6.155×10^{-3}. The equivalent negative resistance was found to be about 18 ohms. The effective resistance of the signal structure was calculated to be 2.51 ohms. The gain was found to be equal to 1.4 or 1.46 db.

V. ANALYSIS AND CONCLUSIONS

The main purpose of the harmonic generator experiment was to make a comparison of the harmonic generating ability of a thin magnetic film and a thin YIG disk. The use of harmonic generators in this frequency range is not as great as at higher frequencies where other types of power sources are not readily available.

For the frequencies considered here the magnetic thin film out-performed the YIG disk. One reason that the YIG disk had a poorer output could be that energy was lost from the uniform precession into spin waves. There are two types of coupling of energy to spin waves. The loss of energy can be caused by the onset of an instability in the motion of the magnetic vector which couples energy exponentially to the spin waves of one-half the resonant frequency. This flood of energy out of the uniform motion prevents the precession angle from increasing and brings about the early onset of the decline of the permeability at resonance. There is usually a threshold for this type of coupling but no threshold was observed in any of the experimental data.

Energy loss can also be caused by irregularities which can couple energy from the uniform mode of precession to spin waves of the same frequency and there is no threshold for this process as energy exchange can take place at all levels

of driving field intensity.

The YIG disk was cracked in the process of placing in the device and also the edges of the disk were sharp. These are two common types of irregularities. The surface of the YIG disk was highly polished so surface irregularities should not have entered in to any extent. Both types of coupling could be present at higher power levels with the coupling loss due to irregularities masking the threshold for the instability.

It was shown by Suhl (25) that when the coupling to spin waves is even as large as 10 percent compared with the direct transfer of energy to the lattice, there is a definite absence of a sharp critical point. There was no sharp resonance point observed in the YIG disk.

A phenomenon which could cause a lower output for the thin magnetic film is skin depth. The conductivity of thin magnetic films is roughly one tenth that of copper. The relative permeability of thin magnetic films is about 740. Using these values the skin depth for a frequency of 1300 mc is approximately 2200 A^{o}. In actual reality this is not the case as the exchange forces in the thin magnetic film have the effect of decreasing the relative permeability at these frequencies. Skin depth is a definite problem though and will be a larger factor as the frequency is increased.

The YIG disk has an extremely high resistivity and

therefore skin depth is not a problem.

There is another problem with the YIG disk that is not found in the magnetic thin film and that is that when the YIG disk is biased to resonance at the frequencies considered in this dissertation, the disk may not be completely magnetized into a single domain. Losses then occur through domain wall motion and are known as low field losses.(12). The demagnetizing factor due to the geometry of the disk should help minimize this effect.

Eddy currents in the stripline at the sample and shielding effects of the stripline are also sources of energy loss. The striplines were slit longitudinally into narrow strips to help minimize these effects.

The greatest improvement in output for both the harmonic generators and parametric amplifiers would result if the Q's of the resonant structures and the coupling between the magnetic material and the resonant structures were improved. At these frequencies cavity type resonators are fairly large and the resulting ratio of the volume of the magnetic material to the volume of the cavity is very small. This results in essentially a poor coupling between the magnetic material and the resonant structure.

To keep the resonant frequency of a coil of wire above the frequencies considered, it was necessary to limit the coil to about 2-4 turns and to space the turns at a small

distance apart. The coils generally resulted in the lowering of the Q of the resonant structure that it was connected to. Therefore very little improvement was realized from substituting a coil of wire for the short piece of stripline. In the harmonic generator the output was greater using the stripline.

The general equation of motion developed here for the parametric amplifier assumes no rotation of the magnetization out of the plane of the material and also assumes that the value of the magnetization vector is constant. For the relatively small values of bias used in the YIG parametric amplifier and for the situation in the thin magnetic film amplifier where the ratio of H_p to $H_B + H_K$ is essentially unity, the general equation of motion developed here is only an approximation. The equation of motion also does not take directly into consideration the loss of energy to spin waves.

The fact that the parametric amplifier consisted of tuned structures was also not taken directly into consideration. The terms at frequencies other than those supported by the parametric amplifier were assumed negligible and were not considered in the driving function and were discarded in the solution. Other methods of representing the parametric amplifier have their disadvantages also. Certain simplifying assumptions must be made and the solutions have certain factors that are not readily measured experimentally. The

equation of motion as developed here has an advantage in that it is relatively simple.

The equivalent circuit is a low frequency model but can be used at high frequencies if the relationship between the magnetic fields and the equivalent currents can be established. The structures were assumed to be tuned so for these frequencies the lump parameter equivalent circuit consisted only of an equivalent resistance. It was assumed that the equivalent reactance component of any structure to a current at a frequency other than the resonant frequency was very large and blocked the current from flowing.

The coupling factor between the input power and the field seen by the magnetic material and the coupling factor between the field generated in the magnetic material and that available at the output terminals were only calculated approximately.

The value of the phenomenological damping constant α used in the calculations of the thin magnetic film amplifier was the value measured at low frequencies. Considering these facts the analytical results did compare quite satisfactorily with the measured results.

The frequencies considered here seemed to be in a mid-ground region. The frequencies are too high to make efficient use of coupling coils and too low to make practical

use of resonant cavities. The frequencies are too high for the magnetic thin film to operate efficiently and too low for the YIG disk to give good results.

VI. LITERATURE CITED

1. Ayres, W. P., P. H. Vartanian, and J. L. Melchor. Frequency doubling in ferrites. Physical Review 100: 1791-1793. 1955.

2. Berk, A. D. Dependence of the ferromagnetic resonance line width on the shape of the specimen. Journal of Applied Physics. 28: 190-192. 1957.

3. Bloom, S. and K. K. N. Chang. Theory of parametric amplification using nonlinear reactances. RCA [Radio Corporation of America] Review 18: 578-593. 1957.

4. Bura, P. The Degenerate and quasi-degenerate mode of parametric amplification. Institute of Radio Engineers Transactions on Circuit Theory, CT-7: 200-210. 1960.

5. Bura, P. Resonant circuit with periodically-varying parameters. Wireless Engineer. 29: 95-100, 120-126. 1952.

6. Conger, R. L. and F. C. Essig. Resonance and reversal phenomena in ferromagnetic films. Physical Review 104: 915-923. 1956.

7. Denton, R. T. Characteristics of a ferromagnetic amplifier using longitudinal pumping. Journal of Applied Physics. 32: 300S-307S. 1961.

8. Fletcher, R. C., R. C. LeCraw and E. G. Spencer. Electron spin relaxation in ferromagnetic insulators. Physical Review 117: 955-963. 1960.

9. Gilbert, T. L. A Lagrangian formulation of the gyromagnetic equation of the magnetization field. (Abstract) Physical Review 100: 1243. 1955.

10. Gillette, P. R. and K. Oshima. Magnetization reversal by rotation. Journal of Applied Physics. 29: 529-531. 1958.

11. Hsiao, K. W. Use of magnetic thin film in microwave parametric amplifier. Unpublished Ph.D. thesis. Library, Iowa State University of Science and Technology. Ames, Iowa. 1962.

12. Landau, L. and E. Lifshitz. On the dispersion of magnetic permeability and ferromagnetic bodies. Physikalische Zeitschrift der Sowjet Union 8: 153-169. 1935.

13. Lax, B. and K. J. Button. Microwave ferrites and ferrimagnetics. McGraw-Hill Book Co. New York, N. Y. 1962.

14. Manley, J. M. and R. E. Rowe. Some general properties of non-linear elements. I. General energy relation. Institute of Radio Engineers Proceedings. 44: 904-913. 1956.

15. McLachlan, N. W. Theory and application of Mathieu functions. Clarendon Press. Oxford, England. 1947.

16. Olson, C. D. and A. V. Pohm. Flux reversals in thin magnetic films of 82% Ni, 18% Fe. Journal of Applied Physics. 29: 274-282. 1958.

17. Pohm, A. V. Switching mechanism in thin ferromagnetic films. (Dittoed) Department of Electrical Engineering, Iowa State University of Science and Technology. Ames, Iowa. 1959.

18. Poole, K. M. and P. K. Tien. A ferromagnetic resonance frequency converter. Institute of Radio Engineers Proceedings. 46: 1387-1396. 1958.

19. Ramo, S. and J. R. Whinnery. Fields and waves in modern radio. John Wiley and Sons. New York, N. Y. 1960.

20. Read, A. A. The theory of thin magnetic film devices. (Dittoed) Department of Electrical Engineering, Iowa State University of Science and Technology. Ames, Iowa. 1962.

21. Read, A. A. and A. V. Pohm. Magnetic film parametric amplifiers. National Electronics Conference Proceedings 15: 65-78. 1960.

22. Slater, J. C. Microwave electronics. Van Nostrand Co., Inc. New York, N. Y. 1950.

23. Smith, D. O. Static and dynamic behavior of thin permalloy films. Journal of Applied Physics. 29: 264-273. 1958.

24. Sokolnikoff, I. S. and R. M. Redheffer. Mathematics of physics and modern engineering. McGraw-Hill Book Co. New York, N. Y. 1958.

25. Suhl, H. The non-linear behavior of ferrites at high signal levels. Institute of Radio Engineers Proceedings 44: 1270-1284. 1956.

26. Suhl, H. Theory of the ferromagnetic microwave amplifier. Journal of Applied Physics. 28: 1225-1236. 1957.

VII. ACKNOWLEDGEMENTS

The author wishes to acknowledge Professor A. V. Pohm for his suggestions, guidence, and encouragements. He also wishes to thank J. T. McConnel and the rest of the shop. To thank C. Comstock and R. A. Sharpe for their help in programing the Cyclone Computer. Thanks to Texas Instruments for supplying a needed piece of equipment. Thanks are also due many other members of the staff at Iowa State University and to Mrs. James Thomas who typed the thesis.

VIII. APPENDIX

If there exists an equation of the form

$$\ddot{y}(x) + a(x)\, y(x) = f(x) \tag{1}$$

then the homogeneous solution is of the form

$$y(x) = Ay_1(x) + By_2(x) \tag{2}$$

A particular solution can be attempted of the form

$$y(x) = v_1(x)\, y_1(x) + v_2(x)\, y_2(x) \tag{3}$$

$\dot{y}(x)$ then can be written as

$$\dot{y}(x) = v_1(x)y_1'(x) + v_2(x)y_2'(x) + v_1'(x)y_1(x) + v_2'(x)y_2(x) \tag{4}$$

The solution will be simplified if $v_1(x)$ and $v_2(x)$ are chosen such that

$$v_1'(x)y_1(x) + v_2'(x)y_2(x) = 0 \tag{5}$$

then

$$y'(x) = v_1(x)y_1'(x) + v_2(x)y_2'(x) \tag{6}$$

and

$$y''(x) = v_1(x)y_1''(x) + v_2(x)y_2''(x) + v_1'(x)y_1'(x) + v_2'(x)y_2'(x) \tag{7}$$

Substituting equations 3 and 7 in 1 results in

$$v_1(x)y_1''(x) + v_2(x)y_2''(x) + v_1'(x)y_1'(x) + v_2'(x)y_2'(x)$$

$$+ a(xv_1(x)y_1(x) + a(x)v_2(x)y_2(x) = f(x) \qquad (8)$$

Equation 8 becomes on rearranging

$$v_1(x)\ (y_1''(x) + a(x)y_1(x)) + v_2(x)\ (y_2''(x) + a(x)y_2(x))$$

$$+ v_1'(x)y_1'(x) + v_2'(x)y_2'(x) = f(x) \qquad (9)$$

but $y_1(x)$ and $y_2(x)$ are solutions of the homogeneous equation

$$y''(x) + a(x)y(x) = 0 \qquad (10)$$

therefore

$$v_1'(x)y_1'(x) + v_2'(x)y_2'(x) = f(x) \qquad (11)$$

Equations 5 and 11 can be solved for $v_1'(x)$ and $v_2'(x)$ resulting in

$$v_1'(x) = \frac{\begin{vmatrix} 0 & y_2(x) \\ f(x) & y_2'(x) \end{vmatrix}}{W}$$

$$v_2'(x) = \frac{\begin{vmatrix} y_1(x) & 0 \\ y_1'(x) & f(x) \end{vmatrix}}{W} \qquad (12)$$

where

$$W = \begin{vmatrix} y_1(x) & y_2(x) \\ y_1'(x) & y_2'(x) \end{vmatrix} = y_1(x)y_2'(x) - y_2(x)y_1'(x) \tag{13}$$

is the Wronskian and is $\neq 0$ since $y_1(x)$ and $y_2(x)$ are linearly independent solutions of $y''(x) + a(x)y(x) = 0$. $y(x)$ can then be represented as

$$y(x) = y_1(x) \int \frac{-y_2(u)}{W} F(u)\, du + y_2(x) \int \frac{y_1(u)}{W} F(u)\, du \tag{14}$$

Since both $y_1(x)$ and $y_2(x)$ satisfy equation 10 then

$$\frac{y_1''(x)}{y_1(x)} = \frac{y_2''(x)}{y_2(x)} = -a \tag{15}$$

Equation 15 can be integrated by parts by letting

$$u = y_2(x)$$

$$dv = \frac{d}{dx}\,(y_1'(x)) \tag{16}$$

then equation 15 becomes

$$y_2(x)y_1'(x) - \int y_1'(x)y_2'(x)dx - y_1(x)y_2'(x) + \int y_2'(x)y_1'(x)dx$$

$$= \text{a constant} \tag{17}$$

Therefore W equals a constant and can be pulled outside the integral sign and equation 14 becomes

$$y(x) = -\frac{y_1(x)}{W}\int F(u)y_2(u)du + \frac{y_2(x)}{W}\int F(u)y_1(u)du \qquad (18)$$